1 Modeling Channel Migration and Floodplain Sedimentation in Meandering Streams

ALAN D. HOWARD
University of Virginia

INTRODUCTION

Meandering streams are one of the few geomorphological systems for which an abundant historical record exists of changes in channel pattern and associated flood-plain erosion and deposition. Despite the evidence from surveys, aerial photographs, topographic mapping, process measurements, dendrochronology and floodplain stratigraphy, geomorphologists and sedimentologists are just beginning to construct realistic process models of meandering stream evolution. The model discussed here combines simulated bank erosion and channel migration with a simple model of floodplain sedimentation. Such simulation modeling has both practical and theoretical utility for prediction of channel and floodplain changes, validation of theoretical process models, and increased understanding of the sedimentological structure of fluvial deposits, with implications for petroleum geology and groundwater flow.

The model discussed here has three major components. The first is a model of flow, bed topography, and sediment transport in meandering streams. This component has been the primary stumbling block in developing simulation models of stream meandering and sedimentation, because appropriate theoretical models have become available during the last decade only. The second component is a relationship between near-bank velocity and depth and corresponding rates of bank erosion and lateral migration. The final ingredient is a process model of floodplain sedimentation. The marriage of a realistic model of meandering with floodplain sedimentation is the novel contribution of this paper.

In the first section the basic structure of the model is presented. Results of some simulations are presented in the second section to illustrate the essential features of the model. The present version of the model is preliminary; the discussion presents possible enhancements and extensions of the model, and research needed to validate and improve such simulation models.

FLOW AND SEDIMENT TRANSPORT MODEL

Since the bank erosion rate is assumed to be related to near-bank flow velocity and depth, an essential element is a mathematical model to predict flow and bed configuration within a sinuous channel. Several such models are available, ranging from linearized one-dimensional (along-stream) models with implicit representation of cross-stream variations in flow, topography, and sediment transport (Johannesson and Parker, 1989; Odgaard, 1989a,b; Parker and Johannesson, 1989) through two-dimensional (downstream and cross-stream) solutions (e.g. Nelson and Smith, 1989a,b). All of these models incorporate simplifying assumptions of the governing equations in order to make numerical solutions feasible. The Johannesson and Parker (1989) model (abbreviated JP) is adopted here, because it captures the essential features of flow, bed topography, and transport in meandering streams, and it is easy to implement and computationally efficient. The JP model is a descendent of the pioneering paper by Ikeda, Parker and Sawai (1981), and it provides good predictions of the bed topography and the flow characteristics in experimental meandering channels with narrow width, vertical banks, and mobile sediment beds. Furthermore, the JP model, when combined with the assumption that bank erosion rates are proportional to near-bank flow velocity, gives accurate estimates of bank erosion rates in natural channels (see later discussion). The Odgaard (1989a,b) model is very similar, and could be investigated as an alternative. In the model, local depth (h) and downstream vertically averaged velocity (u) are resolved into a section mean (H and U) and a dimensionless perturbation (h_1 and u_1) (Figure 1.1):

$$u = U(1 + u_1) \tag{1.1}$$

$$h = H(1 + h_1) \tag{1.2}$$

Generally, we are interested in near-bank values, indicated as u_{1b} and h_{1b}. At the channel centerline u_1 and h_1 are assumed to equal zero. Several simplifing assumptions are incorporated, among which are a spatially and temporally constant channel width and a linear cross-stream variation in the vertically averaged downstream velocity, with negligible sidewall effects on near-bank flows (Figure 1.1a). In other words, the effect of sidewalls on the downstream velocity field is assumed to be important in a narrow zone at the bank only, and the velocity distribution in this zone is not modeled explicitly. The bed and water surface are assumed to be sloping linearly in the cross-stream direction (Figure 1.1b), although the magnitude and direction of the slope vary downstream. Thus the model provides a crude representation of the point bar as a uniformly sloping bed. Furthermore, the energy gradient and average channel depth are assumed to be uniform in the downstream direction. The model predicts the steady-state values of flow, bed topography and sediment transport; therefore, transient bedforms, such as ripples, dunes and migrating transverse bars, are not modeled and their presence is assumed not to introduce systematic effects on local time-averaged depth and velocity. Exposition of the JP model in this paper will be limited to identification of the important model input parameters and local variables and presentation of the governing differential equations. The parameters that are input to the simulation to describe channel and sediment characteristics (Table 1.1) are assumed to be constant areally. Several additional parameters are
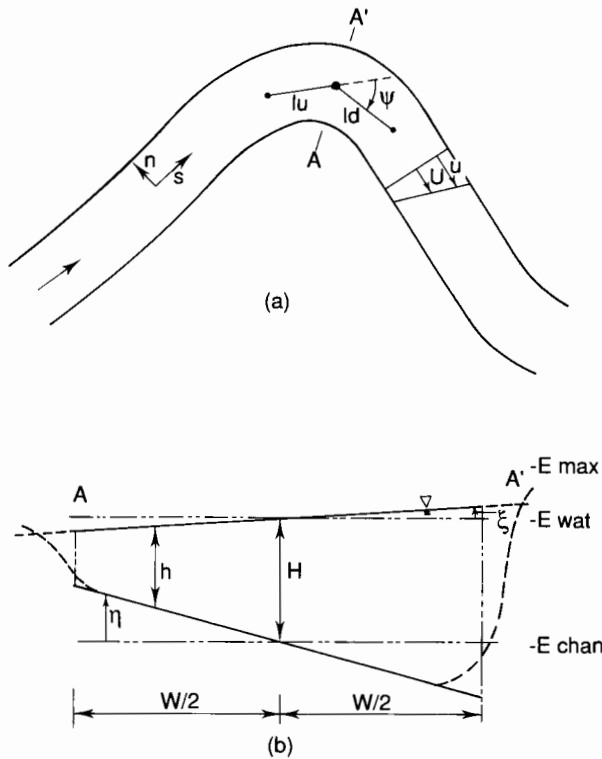
Figure 1.1 Planform (a) and cross-section (b) of a meandering stream showing defini-
tions: (a) cross-stream and downstream coordinate system, downstream vertically
averaged velocity (equation (1.1)), and measurement of channel planform curvature
using centerline nodes to represent the stream (equation 1.16)); and (b) channel depth
(equation (1.2)), bed and water surface elevations (equations (1.A8a) and (1.A8b)), and
reference levels for the depositional model (equations (1.17) and (1.18)). Reference levels
for bed- and water-surface elevations are the average elevations of the bed and water
surface, respectively. The inner and outer near-bank locations shown by vertical long-
short dashed lines. The assumed bed cross-stream profile is shown by the heavy solid
line, and possible actual banks are shown by dashed lines

Table 1.1 Flow and transport input parameters

Parameter	Description
β	Cross-stream slope effect on cross-stream bedload transport $(1.5)^a$
M	Exponent relating velocity to bedload transport rate (5.0)
F_0	Froude Number: $F_0 = U_0/(g\,H_0)^{1/2}$, where U_0 and H_0 are reach-averaged velocity and depth for a straight channel with gradient equal to the valley gradient, and g is the gravitational acceleration (0.5)
γ_0	Channel width/depth ratio: $\gamma = W/H_0$, where W is channel width (20.0)
C_f	Coefficient of friction: $C_f = (u_*/U)^2$, where u_* is the shear velocity (0.01)

[a]Values in parentheses are those assumed for simulations reported here.

Table 1.2 Local variables

Variable	Description
$\mathscr{C}_w = W\mathscr{C}$	Channel planform curvature normalized by width
$\mathscr{C}_{ws} = W\mathscr{C}_s$	Normalized secondary current cell strength
$S_w = S/W$	Downstream distance normalized by width
u_{1b}	Dimensionless near-bank velocity perturbation
h_{1b}	Dimensionless near-bank depth perturbation

derived from the input parameters (Appendix A). Several local variables are calculated by the model for each location along the stream (Table 1.2). The governing differential equations in the JP model and the solution method for calculating the depth and velocity perturbations are presented in Appendix A. In these equations all distances and the channel curvature are non-dimensionalized by the average channel width, W, so that the distance unit is *width-equivalents*.

Discussion of Flow and Transport Model

Flow, sediment transport and bank erosion in natural stream channels occurs over a spectrum of time and spatial scales. Fluvial sediment transport and its associated bedforms can be ordered into a sequence of increasing time-scale of development: (1) motion of individual particles; (2) ripples; (3) dunes; (4) alternate transverse bars; (5) point bars associated with channel curvature and meander development. An increasing spatial scale is generally associated with this sequence. Although not always warranted, mathematical modeling of any given bedform type usually relies on an averaged representation of the effects of the smaller, more transitory bedforms and their associated flow features and sediment transport phenomena. For example, a model of aeolian dune development utilizes sediment transport formulae that predict the integrated particle flux rather than motion of individual particles (Howard *et al.*, 1978). Furthermore, superimposed ripples are incorporated only through their averaged effects on velocity profiles and sediment transport. The JP model predicts the time-independent average values of bed topography and flow in meandering streams forced by channel curvature only, and thus does not treat migrating dunes and alternate bars (although a time-dependent version of the JP model can be used to predict properties of alternate bars in straight channels—Parker and Johannesson, 1989). In particular, the time-independence assumption implies that a completely straight channel of uniform width, gradient and average depth will have a level, planar bed.

The work of Ikeda, Parker and Sawai (1981) showed that flow asymmetries set up by channel curvature imply development of a regular meandering pattern if bank erosion rates correlate with near-bank velocity perturbations; simulations by Howard and Knutson (1984) and those in the present paper (Figure 1.2) demonstrate that the Ikeda model and its descendants imply development of meanders from a channel that is straight except for small perturbations normal to the flow direction. Thus the curvature-forced perturbations of velocity and depth are a sufficient mechanism to cause development of meanders.

However, other models of stream meandering (Parker, 1976; Callander, 1978; Fredsoe, 1978) incorporate the assumption that development of stream meanders are caused by periodic flow asymmetries associated with alternate bars. Observations of meander development in an initially straight gravel channel apparently forced by alternate bars (Lewin, 1976) offer support for this model, at least for wide, gravel-bed streams. However, models of meander evolution relying on alternate bars have two deficiencies as a universal explanation for meandering: (1) they predict a non-
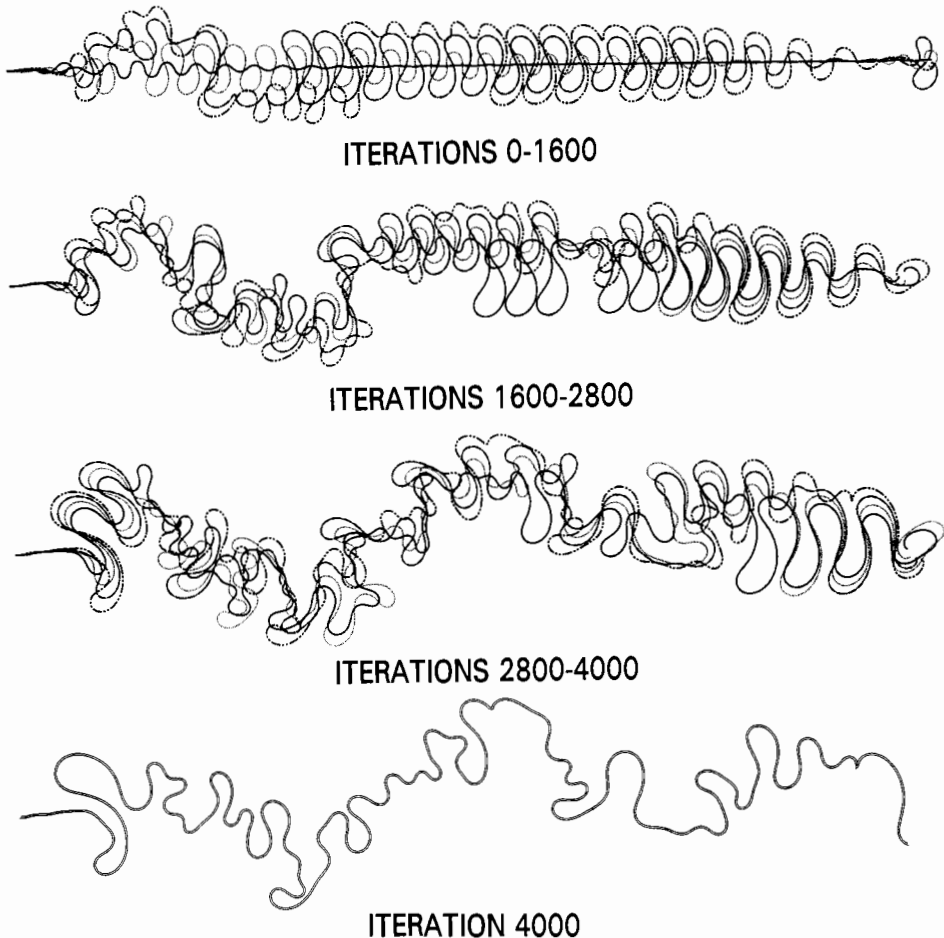

ITERATIONS 0-1600

ITERATIONS 1600-2800

ITERATIONS 2800-4000

ITERATION 4000

Figure 1.2 Evolution of the channel centerline for 4000 iterations using the flow and bed topography model of Johannesson and Parker (1989) coupled with the assumption of bank erosion proportional to the near-bank velocity perturbation, u_{1b} (equation (1.6)), and input parameters from Table 1.1. The simulation starts from a straight stream with small, random normal perturbations, which is not shown but would be an essentially straight horizontal line. Flow is from left to right. In the three top panels the channel centerline is shown at 400 iteration intervals with the sequence solid, dotted, long-dot-dot, and long-short-short lines. In the two central panels the final centerline from the preceding panel is shown as a solid line. The final panel shows the banks of the final channel position

meandering planform for channels too narrow ($\gamma < 10$) for development of alternate bars (the curvature-based model allows meandering under such conditions); (2) although alternate bars can remain fixed in position for specific combinations of flow conditions and cross-sectional geometry, under a range of conditions alternate bars migrate down-channel at a time-scale more rapid than bank erosion rates, at least for streams with cohesive banks.

Therefore, both curvature-forced variations in velocity and depth and alternate bars may control development of meanders. The natural wavelengths of meandering associated with the curvature forcing and alternate bar forcing may not be the same, leading to the possibility of multiple wavelength scales. In many cases migrating alternate bars occur in meandering channels (e.g. Kinoshita, 1961; Fukuoka, 1989; H. Ikeda, 1989; Whiting and Dietrich, 1989; Tubino and Seminara, 1990). Although the present model incorporates the assumption that migrating bars do not affect average bank erosion rates in a systematic manner, such interactions may occur (Whiting, 1990). For certain combinations of width/depth ratio and flow parameters, alternate bars become stationary, and if their natural wavelength is the same as the meander wavelength, a 'resonance' occurs, under which conditions the linearized models, such as JP, predict very large amplitude bars (Blondeaux and Seminara, 1985; Colombini, Seminara and Tubino, 1987; Parker and Johannesson, 1989; Seminara and Tubino, 1989; Tubino and Seminara, 1990). Whether such high-amplitude resonance occurs in natural channels is uncertain at present; non-linear effects may dampen and modify such resonance (G. Parker and W. Dietrich, pers. comm.). Another, and possibly related observation is that alternate bars migrate freely in low amplitude sinuous channels but can become suppressed in high-amplitude sinuous channels, possibly reforming in very high-amplitude meanders (Kinoshita, 1961; Fukuoka, 1989; Tubino and Seminara, 1990; Whiting, 1990). Such locking and suppression may induce systematic variations in flow and bed topography that is not accounted for by the linearized models such as JP, and which could affect bank migration rates (Seminara and Tubino, 1989; Whiting and Dietrich, 1989). This possibility is addressed further in the Discussion section through statistical comparison of the morphometry of simu-lated and natural meanders. Finally, the JP model also is clearly inadequate in the case where the width/depth ratio is great enough ($\gamma \geqslant 40$) for braiding to become important.

In conclusion, the present flow and bed topography model is best suited to channels in which resonant conditions do not occur and where alternate bars, if present, migrate rapidly through the channel in comparison with bank erosion rates. In fact, the JP model appears to be unable to provide a numerically stable solution to flow and bed topography for channels of arbitrary meander planform under conditions close to resonance. The natural conditions most likely to match these restrictions are low width/depth ratio, relatively cohesive banks, and a high suspended-load to bed-load ratio.

BANK EROSION RATE LAWS

Any of four constraints (or processes) may limit the rate of bank erosion. These constraints are, or may be, sequentially linked, so that the slowest among them controls the overall rate.

(1) The rate of deposition of the point bar.
(2) The ability of the stream to remove the bedload component of the sediment eroded from the bank deposits via a net transport flux divergence.
(3) The ability of the stream to entrain sediment from *in situ* or mass-wasted bank deposits.
(4) The rate with which weathering acts to diminish bank sediment cohesion to the point that particles may be entrained by the flow or bank slumping may occur.

Constraint (1) would be limiting for the case where deposition of the point bar were to lag behind bank erosion, so that flow velocities diminish as the channel widens and possibly shallows, with a corresponding decrease in bank erosion until bar deposition 'catches up'. Alternatively, rapid deposition on the point bar might narrow the channel and increase velocities and corresponding bank erosion rates. Neill (1984) related bank erosion to bedload transport rates, which, in part, determines point-bar deposition rates. Observations of rapid bank erosion below cut-offs (Kondrat'yev, 1968; Kulemina, 1973; Brice, 1974b; Bridge *et al.*, 1986) have been suggested to result from efflux of sediment to the next bend (Nanson and Hickin, 1983). However, rapid erosion can also occur owing to high near-bank velocities resulting from the steeper gradients through the cut-off, large curvatures at the cut-offs and changes in bend flow pattern (Howard and Knutson, 1984; Bridge *et al.*, 1986).

Constraint (1) is probably not the limiting factor in most meandering streams. Banks, generally, are more cohesive than the bed so that processes of bank erosion are limiting. Exceptions could occur if the banks are composed of non-cohesive sediments finer in gain size than the channel bed. However, in this case the channel width/depth ratio is likely to be large enough that a braided stream pattern will develop.

The distinctions between constraints (2) through to (4) are subtle but important. Constraint (2) will be the rate limiting factor where the banks are non-cohesive or easily disaggregated and the resulting accumulation of bedload-sized sediment at the foot of banks inhibits further bank erosion until it is removed. The overall rate of bank erosion will thus be related to near-bank flow, sediment transport, and bank height and composition (Hasegawa, 1989a,b). If the banks and slumped bank material are slightly cohesive, the rate of bank erosion will be determined by the detachment capability of the flow (constraint 3), and overall bank erosion rates will be less than if constraint 2 were limiting. If the bank material is strong (e.g. indurated alluvium or rock walls), then erosion by particle entrainment or mass-wasting can be limited by processes of bank disaggregation, such as frost action or chemical weathering, that may or may not be related directly to flow characteristics (constraint 4). It seems likely that all four cases may occur and vary in importance among streams, from place to place along a given stream, and through time at a given location. A variety of processes and material factors that may control bank erosion have been observed, including slumping and toppling (Laury, 1971; Thorne and Lewin, 1979; Thorne and Tovey, 1981; Thorne, 1982; Pizzuto, 1984; Ullrich, Hagerty and Holmberg, 1986; Osman and Thorne, 1988; Thorne and Osman, 1988), freeze-thaw (Wolman, 1959; Lawler, 1986a,b), removal of sediment from the base of the cut bank (Nanson and Hickin, 1986; Hasegawa, 1989a,b), vegetation type and density (Brice, 1964; Pizzuto, 1984; Odgaard, 1987; Hasegawa, 1989a,b), and soil type (Grissinger, 1966, 1982; Turnbull, Krinitsky and Weaver, 1966; Goss, 1973; Murray, 1977). None the less,

fairly simple models relating flow characteristics to bank erosion rates are successful in many stream systems. Overall, the regularity of form and migration pattern of most meandering streams also suggests that fairly simple relationships can be used to predict long-term rates of bank erosion.

One such relationship expresses the bank erosion rate, ζ, as a function of the difference between the near-bank shear stress, τ_b, and the average boundary shear stress, τ:

$$\zeta = \mathscr{E}(\tau_b - \tau)/\tau \tag{1.3}$$

where $\mathscr{E}$ is bank erodibility (units of length per unit time), which may depend upon bank sediment characteristics, flow properties and channel planform shape. This equation can be re-expressed in terms of flow velocities using the definition of shear velocity and the assumed constancy of the coefficient of friction (Table 1.1):

$$(\tau_b - \tau)/\tau = (u_b^2 - U^2)/U^2 \tag{1.4}$$

By definition (1.1)

$$u_b^2 = U^2 (1 + u_{1b})^2 \simeq U^2 (1 + 2u_{1b}) \tag{1.5}$$

where in the right-hand side the squared (higher order) term in the velocity perturbation has been dropped. This results in a linear relationship between bank erosion rate and the velocity perturbation

$$\zeta \simeq 2\mathscr{E}u_{1b} \tag{1.6}$$

This linear relationship between bank erosion and velocity perturbation has been assumed in the models of Ikeda, Parker and Sawai (1981), Beck (1984), Beck, Mefli and Yalamenchili (1984), Parker (1984), Howard and Knutson (1984), Parker and Andrews (1986), Hasegawa (1989a,b), and Odgaard (1987). Hasegawa (1989a,b) shows a strong correlation between observed bank erosion rates and u_{1b} in short stretches of natural meanders. Pizzuto and Meckelnburg (1989) and Odgaard (1987) have made similar observations. Parker (1984) and Furbish (1988) show that the observations of Hickin and Nanson (1975,1984) and Nanson and Hickin (1983,1986) of a direct relationship between mean bend curvature and bank erosion rate in gentle bends is consonant with a proportionality between erosion rate and the velocity perturbation.

Since u_{1b} lags significantly the downstream changes in curvature (Figure 1.3), meanders both migrate downstream and enlarge in amplitude, with eventual neck cut-offs (Parker and Andrews, 1986; Howard and Knutson, 1984; Parker, 1984). However, as individual meander loops increase in amplitude, these models also predict that inflection points tend to become fixed and little downstream migration occurs; this is illustrated in Figure 1.2, in which successive positions of the simple asymmetric loops at the right side of panels 2 and 3 intersect at nearly fixed positions near the inflection points.

Equation (1.6) is probably most relevant to erosion rate being limited by detachment of either *in situ* or slumped cohesive bank sediment (constraint 3). Erosion rates of cohesive sediments are commonly found to correlate with the applied fluid shear force (Parthenaides, 1965; Parthenaides and Paaswell, 1970; Akky and Shen, 1973; Parchure and Mehta, 1985; Ariathurai and Arulandan, 1986; Kuijper, Cornelisse and

Winterwerp, 1989), and Howard and Kerby (1983) found that channel erosion rates in badlands on mudstones and shales were related linearly to bed shear.

However, there is likely to be a critical near-bank shear stress, τ_t, below which bank erosion ceases. This suggests that equation (1.6) should be rewritten as

$$\zeta = \mathcal{E}(\tau_b - \tau_t)/\tau \simeq \mathcal{E}(2u_{1b} - \pi) \tag{1.7}$$

where

$$\pi = \begin{cases} 0 & \text{for } \tau_t \leqslant \tau \\ \dfrac{\tau_t - \tau}{\tau} & \text{for } \tau_t > \tau \end{cases}$$

and erosion occurs for positive values of $(2u_{1b} - \pi)$ only. Since overall channel width is presumably determined by a dominant discharge near bankfull, the value of τ_t would be the average boundary shear associated with that stage. Note that equation (1.7) implies that localized bank erosion would occur at low stages and more generalized erosion at high stages, and that (1.7) is equivalent to equation (1.6) if the dominant discharge is such that $\tau \geqslant \tau_t$.

Odgaard (1989a,b) has suggested that bank erosion is related to the depth perturbation rather than the velocity perturbation. By analogy to equation (1.6)

$$\zeta \simeq 2\,\mathcal{E}h_{1b} \tag{1.8}$$

Odgaard (1989b) presents data that suggests that the depth perturbation is better at predicting the location of first outer bank erosion along bends of the Nishnabotna River, Iowa. Odgaard presents little justification for his erosion model, but mentions the analyses of Osman and Thorne (1988) and Thorne and Osman (1988), which indicate that bank stability decreases with bank height. Nanson and Hickin (1986) found a good correlation between bank erosion rates and the grain size of sediment exposed in the deepest scour holes in meander bends of Canadian rivers, with the implication that deeper bank sediments (representing bedload rather than overbank deposition) are less cohesive and therefore entrained more readily. Lapointe and Carson (1986) feel that bank erosion near the beginning of bends is related more to great depth rather than high velocity.

There is an important consequence to patterns of meander evolution if erosion rates are related to h_{1b} rather than u_{1b}. For flow and sediment characteristics that are typical of natural stream channels, the depth perturbation is nearly in phase with, or may even lead the curvature (Figure 1.3). This implies that meanders would tend to grow in amplitude, with negligible downstream migration.

Hasegawa (1989a,b) provides an analysis of the factors controlling bank erosion if transport of eroded bank sediment (constraint 2) is the limiting factor. Six terms related to transport rate, sediment characteristics, flow properties and bank geometry emerge from his analysis (Hasegawa, 1989a, his equation 8). Three of the terms are of second-order importance only, and the remaining three can be summarized as follows for conditions where sediment transport rate is well above threshold conditions:

$$\zeta = \mathcal{E}(u_{1b} - h_{1b}/2 - H_b/3H) \tag{1.9}$$
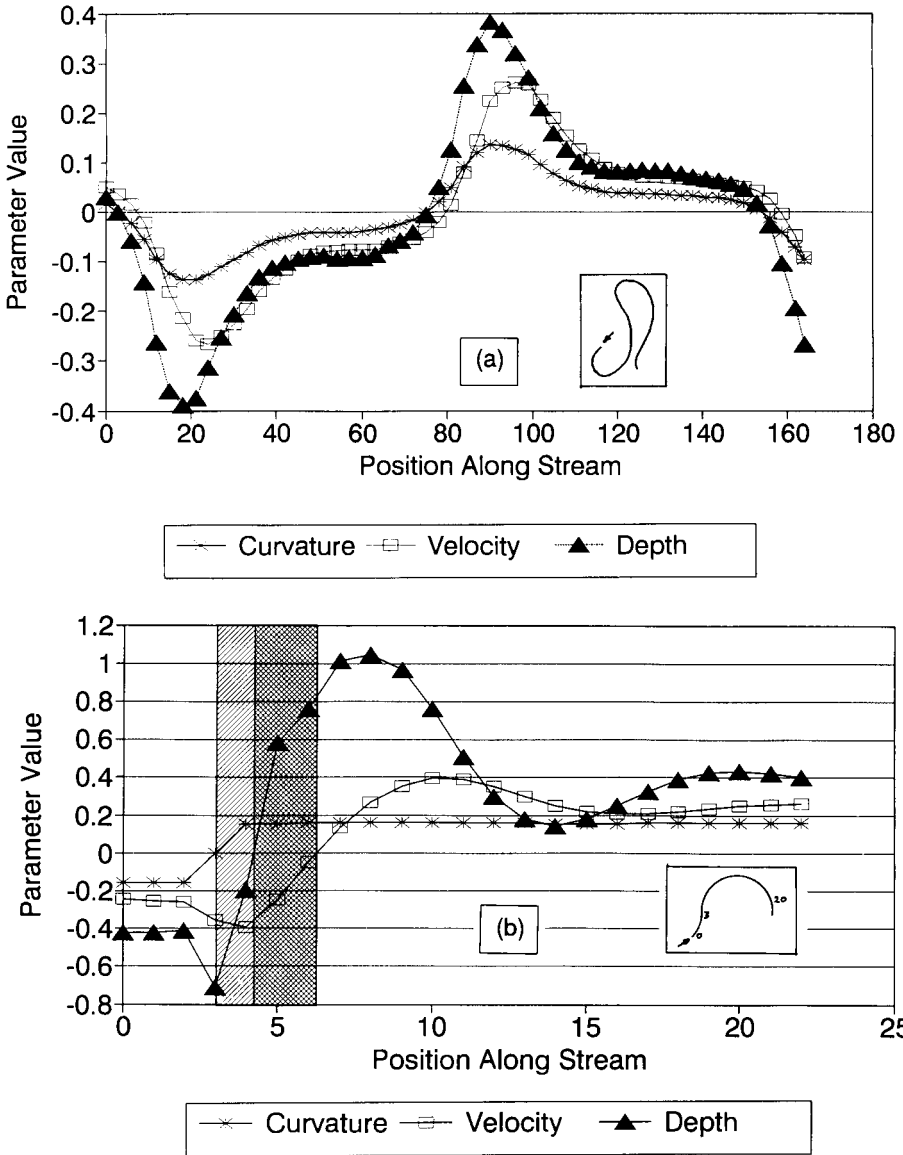
Figure 1.3 Local channel curvature and near-bank velocity and depth perturbations in meanders as predicted by the Johannesson and Parker model (1989) using parameters from Table 1.1. X-axis is position in bend measured downstream in width-equivalent units. Curvature is width-normalized; (a) a large asymmetric meander such as occurs in iterations 1600–2800 near the right-hand side of Figure 1.2; the channel planform is shown in inset; (b) a meander with an abrupt change of sign of curvature, with planform shown in inset. In (b) the initial velocity and depth perturbations are close to equilibrium values for constant curvature. Note the overshooting effects in the near-bank depth and velocity responses to curvature change. Ruled and cross-ruled areas delineate the zone along the stream in which the curvature and velocity perturbations have opposite sign and bank erosion is directed towards the inner, convex bank if it is proportional to the near-bank velocity perturbation u_{1b}. The cross-ruled area shows the zone in which the depth and velocity perturbations have opposite sign

where ζ is the rate of bank erosion, $\mathscr{E}$ depends upon bank sediment characteristics and transport parameters, and H_b is the height of the bank above water level. Hasegawa suggests that the third term will be of smaller magnitude than the other two and can be neglected. However, where a stream impinges on a tall bank of non-cohesive sediment (e.g. a terrace) the emergent bank height would become important. Hasegawa (1989a) also suggests that depth perturbation (second term) 'does not directly arrest erosion, but rather works only to decrease the erosion rate' and 'can be left out of consideration' (p. 226). However, this reasoning is counter to his analysis, which suggests that h_{1b}, the magnitude of which may exceed u_{1b} in tight bends, is of direct importance. Inclusion of the depth perturbation term may indeed have important effects on patterns of bank migration, because the depth and velocity perturbations are out of phase (Figure 1.3). The negative weighting of depth in Hasegawa's relationship (opposite to the positive weighting in Odgaard's model) is a result of the greater amount of sediment contributed from higher banks, and its effect would be to shift the locus of maximum erosion downstream from the locus of maximum near-bank velocity, thereby increasing the ratio of rates of downstream meander migration to meander enlargement.

Where erosion rates are limited by disaggregation processes (constraint 4) acting on the channel banks (such as frost action, wetting and drying, or progressive bank failure), erosion rates may have an upper limit that is independent of the local flow perturbation.

Thus there is considerable uncertainty concerning an appropriate form for the bank erosion relationship. A general relationship is suggested here that includes weighted values of both the depth and velocity perturbation

$$\zeta \simeq 2 \, \mathscr{E} \, (a u_{1b} + \varepsilon h_{1b}) \tag{1.10}$$

where the weight α is probably positive, and ε may be positive, negative, or zero. If very high emergent banks occur locally, an additional term may be included.

Bank erodibility $\mathscr{E}$ may depend upon a number of factors, including bank sediment characteristics, processes determining the rate of bank disaggregation and bank height. Hasegawa's (1989a,b) analysis for transport-limited bank erosion indicates a dependency on sediment density, friction angle, and porosity as well as transport stage. Hickin and Nanson (1984) and Nanson and Hickin (1986) relate bank erodibility to median grain size, d, of sediment at the base of cut banks and the ratio of stream power to bank height. This suggests that

$$\mathscr{E} = \frac{\tau \, \gamma \, U}{\mathscr{F}(d)} \tag{1.11}$$

where $\mathscr{F}(d)$ is an empirical bank resistance function (units of shear stress) that has a form similar to the classic critical tractive force diagrams. Nanson and Hickin (1986) feel that their results are consistent with transport of eroded sediments (constraint 2) being the rate-limiting process. Hasegawa (1989a,b) finds an inverse relationship between measured penetration resistance of banks and bank erodibility. Bank erodibility also may be a function of type and density of bank vegetation.

The present simulation model utilizes equation (1.10) to predict bank erosion rates, with $\alpha = 1$ and $\varepsilon = 0$, in accord with most previous models of bank erosion.

SIMULATION PROCEDURES FOR CHANNEL MIGRATION

The simulation procedures for the bank erosion and channel migration component of the model are similar to those adopted by Howard and Knutson (1984). A number of simplifying assumptions are made, including (1) constant bank erodibility, $\mathscr{E}$, (2) uniform width-averaged sediment load, (3) slow enough bank migration so that the erosion by individual flow events can be represented by a continuous process, (4) a single thread channel with spatially and temporally constant width, and (5) constant input of water and sediment from upstream and a constant downstream base level, so that the stream is not aggrading or downcutting. The *valley* gradient is assumed to be constant, so that the average *channel* gradient is inversely proportional to sinuosity, $\mathscr{T}$. The input parameters β, M, C_f and W are assumed to be constant temporally, but the depth, width/depth ratio, mean velocity and Froude number must be corrected for changing sinuosity:

$$H = H_0 \, \mathscr{T}^{1/3} \tag{1.12}$$

$$\gamma = \gamma_0 \, \mathscr{T}^{-1/3} \tag{1.13}$$

$$U = U_0 \, \mathscr{T}^{-1/3} \tag{1.14}$$

$$F = F_0 \, \mathscr{T}^{-1/2} \tag{1.15}$$

where H_0, γ_0, and F_0 are the values for a straight channel with a gradient equal to the valley gradient, S_0 (the above follow from the relationships $\tau = \varrho g H S = \varrho u_*^2$, $C_f = (u_*/U)^2$, and $\mathscr{T} = S_0/S$).

The simulation proceeds by repeated iterations, each iteration proceeding downstream through the individual points, or nodes, that represent the channel centerline. Individual nodes have a nominal downstream spacing of one width-equivalent. At each node the local near-bank velocity and depth are calculated by the procedures outlined in Appendix A. Local dimensionless curvatures $\mathscr{C}_w$ (Table 2) used in these procedures are calculated by

$$\mathscr{C}_w = 2 \, W \, \Psi/(l_u + l_d) \tag{1.16}$$

where Ψ is the angular change in direction (positive for clockwise downstream turning) at the node and l_u and l_d are the distances to the adjacent upstream and downstream nodes. As the stream migrates, the distance between individual nodes may increase or decrease, necessitating addition or removal of nodes, as discussed by Howard (1984) and Howard and Knutson (1984).

Each point is moved, corresponding to bank erosion and channel migration, by an amount proportional to ζ. This erosion is directed normal to the stream centerline (in the $\vec{n}$ direction, Figure 1.1), moving the centerline to the left (facing downstream) if ζ is positive, and to the right if ζ is negative (in the JP model the near-bank depth and velocity perturbations are equal in magnitude and opposite in sign on opposing banks). Owing to the weighting of upstream curvatures implied by the governing equations, this erosion may be contrary, locally, to the direction of the local curvature.

When separate portions of the channel centerline approach closer than a predetermined distance, a neck cut-off occurs by deleting the points representing the abando-

ned channel. The program checks for potential neck cut-offs each 50 iterations only, so that the critical distance is set to 1.2 widths to minimize the occurrence of channel overlaps. Chute cut-offs and avulsions are not incorporated in the present model.

DEPOSITION MODEL

Major physiographic features in meandering streams include point bars, natural levees, crevasse splays, back swamps, overbank channels, and abandoned channel segments. In the present model, levees, point bars, back swamps and channel fills are modeled as an additive combination of two processes, point bar deposition and overbank sediment diffusion.

Bridge (1975), Jackson (1976), Allen (1977), and Willis (1989) have pioneered models coupling meander migration with depositional facies modeling. These studies have been concerned primarily with stratigraphy and sedimentology of point bars, and have relied on simple idealizations of translation and enlargement in single bends. Here, a more general model of meander migration is used and long-term evolution of floodplain deposits is considered. However, no attempt is made here to model sedimentary facies of the floodplain sediments. Leeder (1978) and Bridge and Leeder (1979) have modeled sedimentary facies deposited by streams in depositional basins, including the effects of avulsions. However, these models do not attempt detailed reconstruction of topography or sedimentary facies within meander belts. The present modeling thus falls in temporal and spatial scales in between the detailed point bar models of Bridge (1975) and others and the basin modeling of Leeder (1978) and Bridge and Leeder (1979). Enhancements of the present approach would be suitable for examination of the sedimentological structure of meander belts.

In accord with observations and theory (Kesel et al., 1974; Pizzuto, 1987), deposition of the coarse fraction of suspended load is modeled as a processes of diffusion from the main channel, with rates decreasing with distance from the channel. However, fine sediment deposition is modeled as slow settling from quiescent flow that is assumed to be independent of location. Several studies also have shown that floodplain deposition rates in meandering streams decrease with floodplain age (Wolman and Leopold, 1957; Everitt, 1968; Nanson, 1980), presumably because older floodplain locations are higher (and thus less frequently and less deeply flooded) and generally farther from the stream channel. Accordingly, deposition rate, Φ, is modeled as a function of relative floodplain height, the rates of fine sediment deposition, and a characteristic diffusion length scale:

$$\Phi = (E_{\max} - E_{\text{act}}) \left[\nu + \mu \exp(- D/\lambda) \right] \tag{1.17}$$

where $E_{\max}$ is a maximum floodplain height, E_{act} is the local floodplain height, ν is the position-independent deposition rate of fine sediment, μ is the deposition rate of coarser sediment by overbank diffusion, λ is a characteristic diffusion length scale, and D is the distance to nearest channel (both measured in channel-width equivalent units). This model is assumed to provide a crude representation of both deposition very close to the channel (banks and levees) as well as more distant overbank sedimentation.

Deposition of the point bar by the migrating channel is accounted for by making the initial floodplain elevation prior to overbank deposition equal to the near-bank channel-bed elevation, η_b (Figure 1.1). Specifically, when migration results in a channel migrating into a floodplain cell, the elevation is reset to the mean channel bed elevation E_{chan}. However, when the channel subsequently migrates past the flood-plain cell, the elevation E_{act} is initially set equal to

$$E_{act} = E_{chan} + \eta_{1b}\, H \qquad (1.18)$$

where E_{wat} is an assumed mean water surface elevation and η_{1b} is the near-bank perturbations of depth below E_{wat} (see Appendix A) for the bank opposite the direction of migration. Note that H equals ($E_{wat} - E_{chan}$). The three elevations E_{chan} < E_{wat} < E_{max} are parameters input to the model (Figure 1.1). Elevations are measured relative to the local E_{chan} and do not account for the valley gradient. Note that equation (1.18) is applied to the newly vacated cell prior to calculation of sediment deposition (equation (1.17)).

Floodplain stratigraphy and sediment composition are not modeled explicitly. Floodplain elevations and ages are stored in a matrix that overlies the meander belt. In the present simulations, each matrix cell corresponds to a square area with sides equal to one width-equivalent.

In summary, the depositional model incorporates both a crude model of point bar sedimentation expressed as a variable advancing bank initial elevation (equation (1.18)) and a bank and overbank depositional component (equation (1.17)).

SIMULATION RESULTS

Figure 1.2 shows the planform evolution of the centreline of a meandering channel simulated with the present model, starting from a stream that is straight except for small, random normal perturbations. Model input parameters are given in Table 1.1. The length of the simulated valley section (and the initial stream length) is 512 widths. The resulting pattern of channel evolution and cut-off development is similar to that obtained by Howard and Knutson (1984) using the earlier flow model of Ikeda, Parker and Sawai (1981).

The initial pattern of migration is very regular and develops the classic 'Kinoshita' loop shape, which is skewed upstream and increases to considerable amplitude prior to cut-off. This is a shape that is characteristic of the solutions to the governing equations (Parker, 1984; Parker and Andrews, 1986) and common in natural streams (Carson and Lapointe, 1983). There are local differences in rapidity of initial growth that depend upon the random perturbations of the initial input stream. However, after cut-offs begin, the stream pattern becomes much more varied in form of meanders owing to the disturbances that propagate throughout the meander pattern as a result of cut-offs. At these advanced stages, the pattern becomes much more similar to natural meandering streams, with their commonly complex loop shapes. As a result of chance occurrence of two or more cut-offs on the same side of the valley, the overall meander belt can develop a wandering path, as noted by Howard and Knutson (1984). The sharp bends that result from cut-offs are very rapidly converted to more gentle bends, commonly by reverse migration caused by maximum flow

velocities occurring on the inside of very sharp bends. The development of varied meander forms from an initially regular pattern indicates that the combination of meander growth, the occurrence of cut-offs, and the influence of complicated initial and boundary conditions (including variations in bank resistance that are held constant) implies a 'sensitivity to initial conditions' in the meandering process. That is, small differences in initial geometry or boundary conditions between two otherwise identical streams will cause different meander patterns. Also, predictability of future meander pattern decreases with time and past river patterns become increasingly uncertain with elapsed time (unless topographic or stratigraphic evidence is available).

The deposition model is illustrated in Figure 1.4, which portrays the evolution of a square region (dimensions of 100×100 width-equivalents) extracted from the middle of a simulated stream approximately five times longer than the square region. Although simulation parameters are the same as those for Figure 1.2, slightly different initial conditions resulted in a different pattern of meander evolution. The simulation starts with an existing meandering stream and shows bank erosion and sedimentation occurring during the course of 2100 iterations. Contours of floodplain age (measured in iterations) are shown in Figure 1.4a. The resulting patterns of meander-loop growth afford examples of most of the types discussed by Brice (1974b) and Hickin (1974). Some portions of the floodplain have not been occupied by the meandering channel during the simulation (outside the dashed lines). Floodplain elevations for two values of the parameter μ, controlling the rate of overbank deposition by sediment diffusion, are shown in Figure 1.4b and 4c. The assumed value is -10 for E_{chan}, 11 for E_{wat} and 20 for E_{max} (arbitrary units).

Similarly, Figure 1.5 shows meander and floodplain evolution for confined meanders developed between non-erodible valley walls. Note that the meanders develop a characteristic asymmetric pattern, with gentle bends terminating abruptly in sharp bends at valley walls, similar to natural confined meanders (Lewin, 1976; Lewin and Brindle, 1977; Allen, 1982; Howard and Knutson, 1984).

Figure 1.6 shows the average relationship between floodplain elevation and floodplain age for the simulations shown in Figure 1.4. As would be expected from the model assumptions, deposition rates decrease with increasing age of the floodplain (or alternatively, with increasing elevation of the floodplain).

These simulations exhibit many of the essential features of natural meandering streams, including overbank deposits gradually increasing in elevation away from the channel, rapid isolation of abandoned channels by filling near the main channel (modeled here as resulting from sediment diffusion from the main channel, but in natural channels advectional transport through the abandoned channel also would occur), and slower infilling of oxbow lakes primarily by deposition from suspension. Note that two neck cut-offs have occurred at the left edge of Figure 1.4 just prior to the end of the simulation, so that the abandoned channels have not been closed by sedimentation, as has occurred for the loops abandoned earlier in the simulation on the right side. Also, the sharp change of curvature at the site of the cut-offs has not yet been smoothed out by rapid meander growth at the cut-off site. There is considerable variability of channel migration rates from bend to bend, and the slope of floodplain surface in the interior of bends is generally steeper the slower the migration (compare Figures 1.4a and 1.4b). For higher rates of overbank deposition most of the floodplain
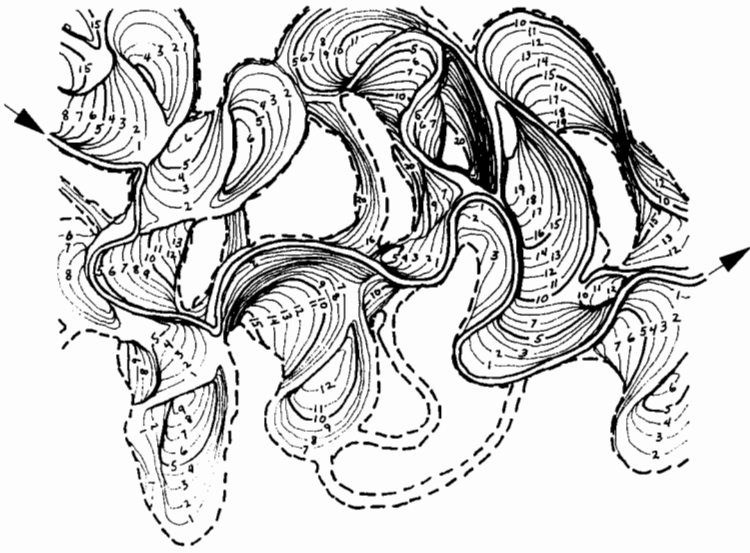
(a) AGE (HUNDREDS OF ITERATIONS)

(b) ELEVATION - LOW OVERBANK DEPOSITION RATE

Figure 1.4 Simulations of floodplain evolution in a freely meandering stream for 2100 iterations; (a) contours of floodplain age, in hundreds of iterations. Location of present stream is shown by arrows and lines delineating its banks. Floodplain areas older than 2100 iterations are bordered by dashed lines and are uncontoured; (b) contours of

rapidly reaches values close to E_{max} and cut-offs are rapidly isolated into oxbows (Figures 1.4c and 1.5c). Both simulations have low values for floodplain sedimentation, v, so that oxbow lakes are filled very slowly.

The simulations with a low rate of overbank sedimentation (Figures 1.4b and 1.5b) exhibit a depositional feature that is a consequence of out-of-phase relationships between near-bank velocity and bed elevation perturbations. Where curvature changes abruptly downstream the depth adjusts quite rapidly on the new outer bank, and generally overshoots its value for constant curvature, but velocity responds more slowly (Figure 1.3b). In this figure the curvature changes at position 3 from negative to a constant positive value. In the zones indicated by ruling and cross-hatching the velocity perturbation is opposite in sign to the curvature, indicating that the highest velocity is directed towards the inside of the bend, where, from equation (1.10), bank erosion will occur. In addition, in the cross-hatched zone, the depth perturbation is positive, so that the depth is greatest on the outside bank. This means that, from equation (1.18), deposition on newly created floodplain on the outside bank must start from very low relative elevations (a scour hole). This zone of very low initial elevations is short (about 2.5 width-equivalents). Just downstream from the cross-hatched zone the velocity perturbation is positive, indicating that the more normal pattern of erosion is directed towards the outer bank. In this zone the depth perturbation is positive and large in magnitude, so that the point-bar elevation on the inner bank is large; therefore, from equation (1.18), floodplain deposition starts from
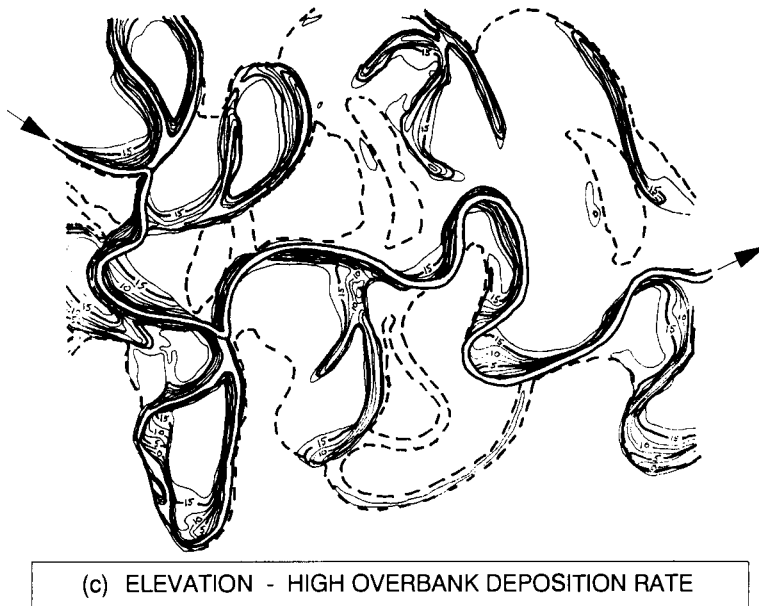

(c) ELEVATION - HIGH OVERBANK DEPOSITION RATE

Figure 1.4 *(cont.)* floodplain elevation for depositional parameters having the values $\lambda = 3$ width-equivalents, $v = 0.0003$ vertical units per iteration, and $\mu = 5v$. Location of low-elevation sloughs indicated by lines from 'S' boxes. (c) Contours of elevation for $\lambda = 3$, $v = 0.0003$, and $\mu = 50v$
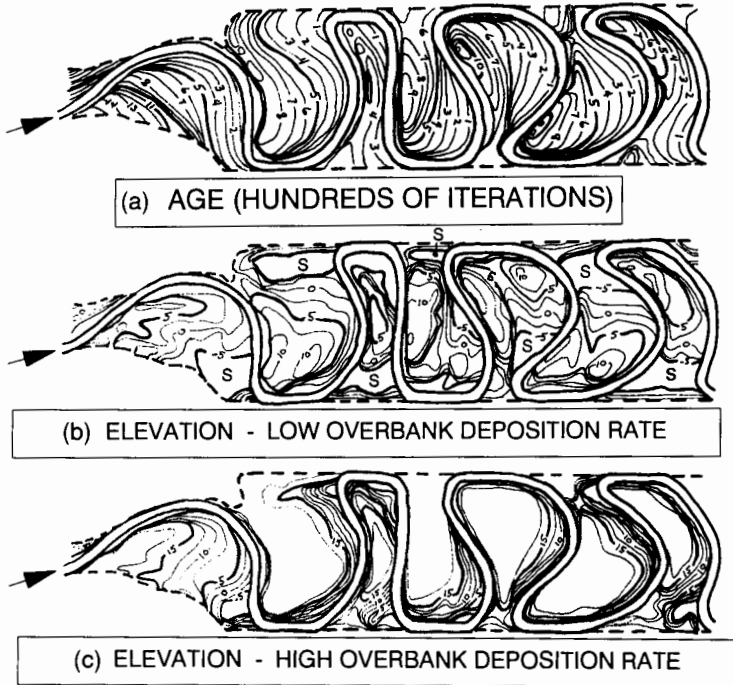
Figure 1.5 Simulations of floodplain evolution of meanders confined within a valley 24 width-equivalents across. Low elevation sloughs are indicated in (b) by 'S'. See Figure 1.4 for further information

a high relative level. Similar effects can occur in narrow zones where curvature either increases or decreases abruptly, but it occurs most strongly where curvature changes sign abruptly.

The simulation modeling indicates that these short zones with lower than average initial floodplain elevations are located in consistent positions relative to bends as the channel migrates, in places leaving behind depressions, or sloughs, in the floodplain deposits. These sloughs are most commonly located in the axial position of sharp meander bends, and are best developed on the downstream end of the point bar near the curvature inflection leading to the next bend. Several of these depressions are labeled with 'S' in Figures 1.4b and 1.5b. These floodplain depressions exhibit several consistent patterns.

(1) The depressions are best developed at strong changes in curvature, which in both simulated and natural streams occurs generally at short, abrupt bends. Such abrupt bends are best developed near the site of recent neck cut-offs (Figure 1.4) or where meander migration is confined by valley walls (Figure 1.5). Long meander bends of the classic Kinoshita form have little lag between velocity and depth perturbation (relative to bend length) and negligible zones in which the sign of these perturbations are opposite and large in magnitude (Figure 1.3a).

(2) Natural and experimental channels abound in similar features, which may result from a mechanism similar to that incorporated in the model. Figure 1.7 shows
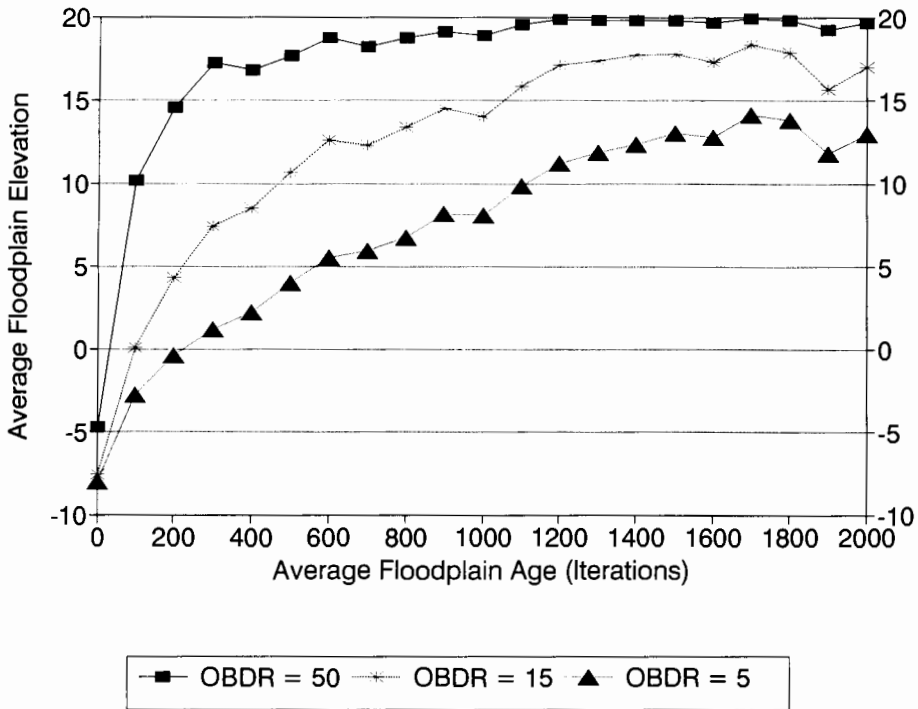
Figure 1.6 Average relationship between floodplain age and floodplain elevation for simulations with three values of the model paramter, μ (overbank deposition rate, OBDR, expressed in multiples of the parameter v). The curves for OBDR = 50 and OBDR = 5 correspond to the simulations shown in Figures 1.4b and 1.4c, respectively

depth contours for two of the experimental runs of Friedkin (1945). Figures 1.8a and 1.8b show natural meandering channels with such sloughs or floodplain depressions. The present modeling suggests that they are best explained simply as sites of retarded deposition owing to the low initial near-bank bar elevations, as noted by Wolman and Brush (1961). Fine sediments accumulating in such sloughs and floodplain lows have been called concave bank benches (Cary, 1969; Taylor and Woodyer, 1978; Woodyer, 1975; Hickin, 1979; Nanson and Page, 1983). Lewin (1978) attributes floodplain sloughs extending upstream from the outside bank of confined and unconfined sharp bends to formation as residual depressions from migrating deep scour pools—essentially the same mechanism as occurs in the simulations (Figures 1.4b and 1.5b).

(3) In the type of sharp bends associated with slough development, large depth perturbations on the inside bank tend to occur in initial portions of the bend, leading to high bars. Since the depth perturbation diminishes through the bend, a typical bar form emerges that is high on the upstream end, diminishing in height downstream and toward the inside of the bend, and terminating in the slough. The sloughs are commonly deepest at their downstream end and shallow or disappear upstream. See the laboratory channels in Figure 1.7 and the natural channel in Figure 1.8b. In some cases in both the simulations and natural channels these
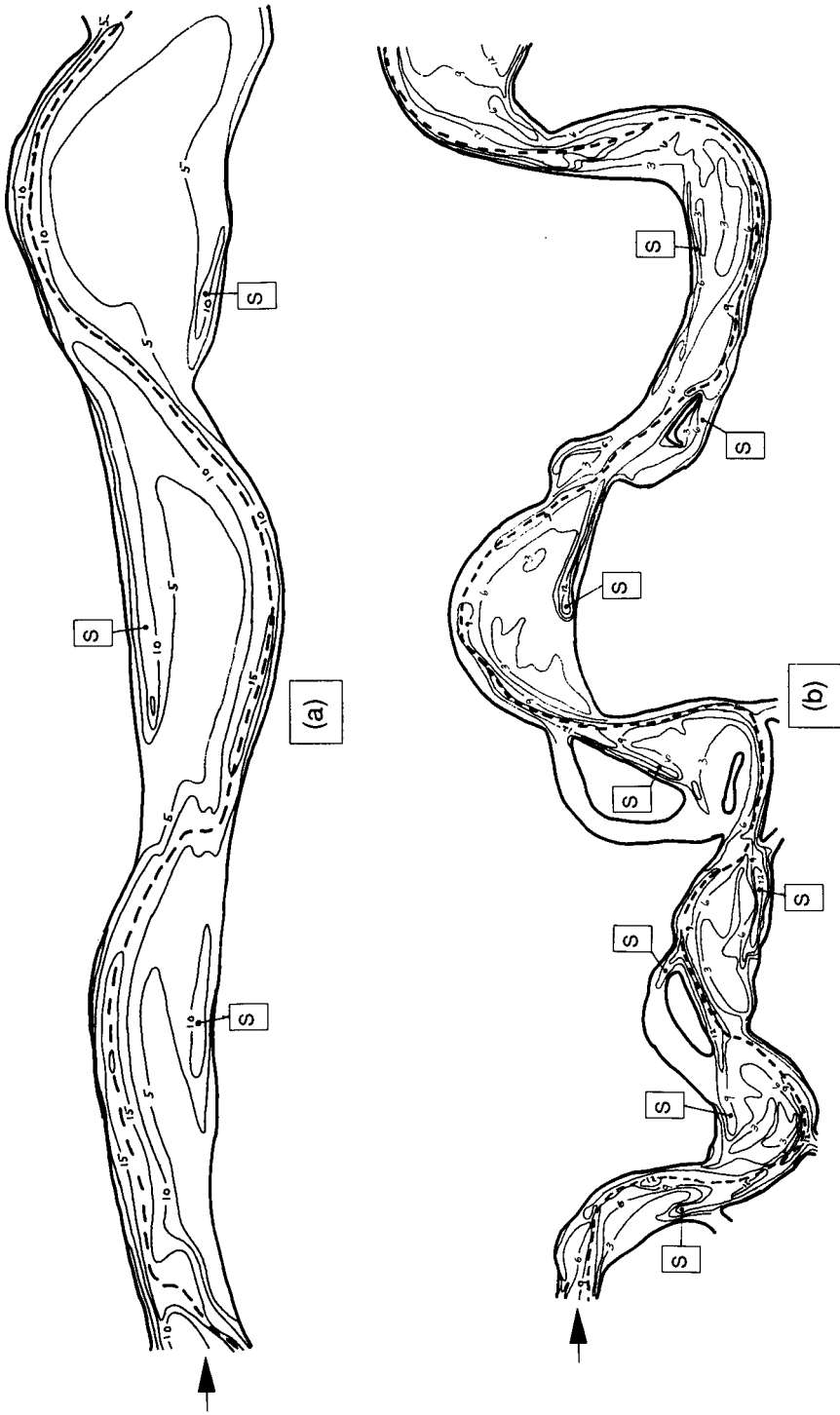
Figure 1.7 Channel and bank elevations for two laboratory meandering channels (Friedkin, 1945). Channel thalweg shown in dashed lines and sloughs are indicated by 'S'. Flow is from left to right; (a) bank stabilization test 5 with relative depths below banks in hundredths of feet. Note prominent near-bank sloughs opening downstream; (b) bank stabilization test 6 with relative depths below banks in hundredths of feet. This run models bank erosion of a portion of the Mississippi River. Note sloughs and mid-channel islands

sloughs may extend completely through the meander axis, creating a second channel and a mid-channel bar (Figure 1.8 (a and c)). The depositional mechanisms modeled here may thus offer an explanation for these commonly occurring bars (Leopold and Wolman, 1957; Hooke, 1986; Bridge *et al.*, 1986). However, natural bars in meandering channels are influenced by flow through the slough, which is not modeled in the present simulations.

(4) The model suggests that these sloughs and bar forms are best developed in streams where depth perturbations are large (high sinuosity and small values of the parameter β governing the slope of point-bars) and where suspended sediment deposition rates are modest (Nanson and Page, 1983). If this is not the case, then bank and floodplain deposition is more uniform (Figures 1.4c and 1.5c).

(5) The simulations suggest that these bar and low floodplain features of wide meandering streams cannot be understood solely in terms of adjustments of bar form to contemporary flow and sediment transport, but are in addition intimately related to the kinematics of bank migration.

(6) The sloughs should be preferred locations for the development of chute cut-offs. Since the sloughs are fixed in location, as the bend sinuosity increased during migration of the main channel the sloughs become more advantageous as a flow route. This is supported by observations by Lewis and Lewin (1983) that chute cut-offs are most common in tight bends and at axial locations (where the sloughs are best developed).

The present explanation for these floodplain depression, sloughs and mid-channel bars may conflict with the dominant current interpretation that these forms result from migration of and deposition from alternate bars coupled with channel migration (Lewin, 1976; Bridge, 1985; Bridge *et al.*, 1986). Alternate bars typically have their highest point located away from the bank with a corresponding depressed zone immediately adjacent to the bank. Such a form is observed in natural channels (e.g. Kinoshita, 1961; Bluck, 1976; Lewin, 1976), flume experiments (Wolman and Brush, 1961; Whiting, 1990), and in the simulations of Nelson and Smith (1989a,b) and Shimizu and Itakura (1989). Bridge (1985) and Bridge *et al.* (1986) suggest that point and mid-channel bars, as well as associated depressions resulting in sloughs, are created from portions of migrating alternate bars that become fixed (or trapped) as the channel shifts owing to bank erosion. However, the JP model does account for sediment continuity and thus predicts time-averaged depositional effects of migrating alternate bars during channel shifting. The question that remains to be resolved is whether the development of fixed point and mid-channel bars and associated depressions are primarily related to transitory effects of migrating bars interacting with channel shifting (and thus not represented in the present model) or are adequately represented by the shifting steady-state bed topography of the JP model. In conclusion, bar sedimentation simulated using the JP model provides a sufficient, if not necessarily accurate, explanation for development of sloughs and mid-channel bars.

The simulations shown in Figures 1.4 and 1.5 show little tendency towards formation of natural levees. A number of other simulations with widely varying values of the deposition parameters in equation (1.17) likewise exhibited no obvious natural levees. One explanation may be the inclusion in the model of decreasing sedimentation rate
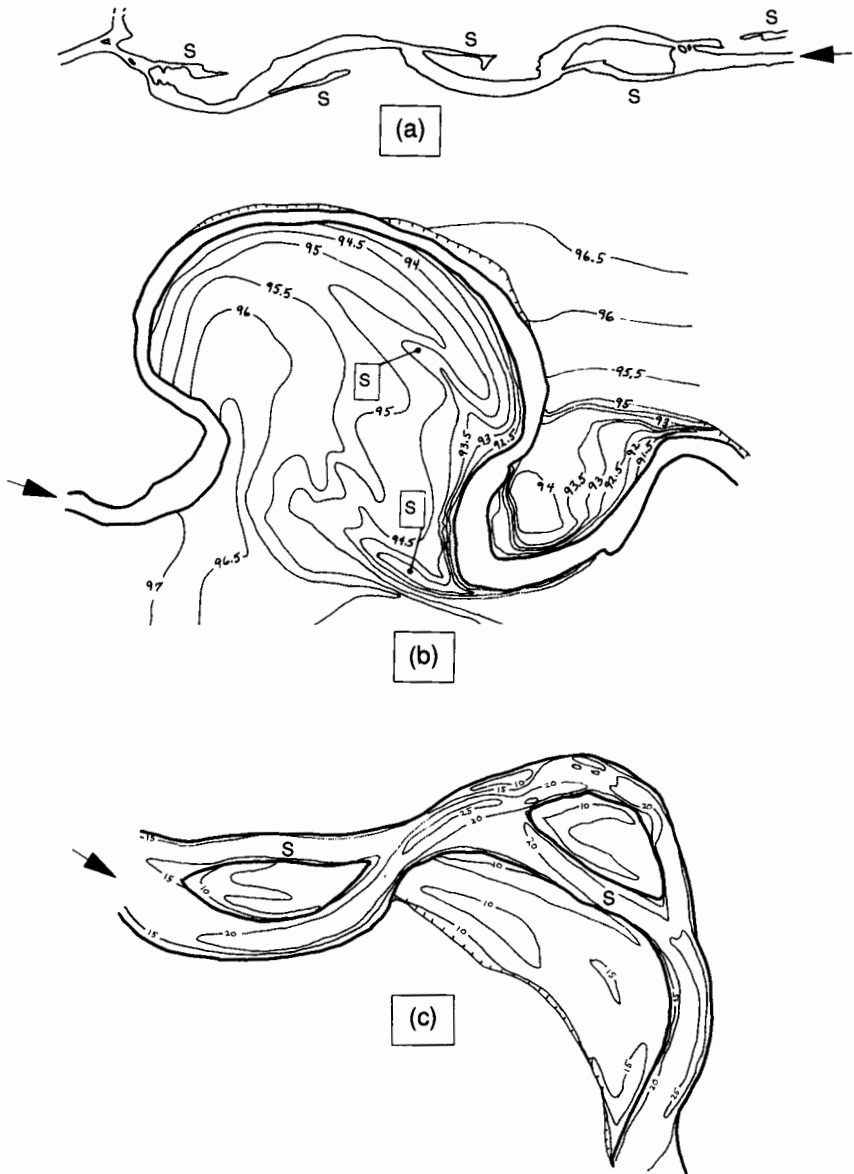
Figure 1.8 Natural channels with sloughs and mid-channel bars, with sloughs and floodplain depressions marked with 'S'; (a) channel banks of a partially confined river, showing prominent sloughs and mid-channel island (modified by permission from Lewin, 1976); (b) floodplain elevations (in feet) for two bends of Watts Branch, Maryland, showing linear depressions extending upstream across point bars from sharp bends (reproduced by permission from Wolman and Leopold, 1957); (c) relative depths (in feet) and banks of two bends of the Calamus River, with thalweg indicated by dashed line (reproduced by permission from Bridge *et al.*, 1986). Note mid-channel bars at bend apices

with increase of surface elevation, including the upper limiting elevation $E_{\max}$. However, simulations with a very high distance-dependent deposition rate, μ, small diffusion distance, λ, and low ν (equation (1.17)), which give average floodplain elevations well below $E_{\max}$, fail to produce levees. Alternatively, pronounced natural levees may occur only in situations where channel beds aggrade relative to their floodplains, so that the difference in near-channel and remote sedimentation rates accumulates through time.

DISCUSSION: PROPOSED MODEL ENHANCEMENTS

The present model could be revised in several ways to improve the fidelity to natural processes and increase the range of environments and features included in the simulation.

Flow and Sediment Transport Model

Improvements in the flow and bed topography model might address the limitations noted earlier. The linear model of Odgaard (1989a,b) represents the point bar by a convex bed profile that is more realistic than the straight-line profile of the JP model. Two-dimensional models of flow and transport are available that operate on the alternate bar time–space scales (e.g. Nelson and Smith, 1989a,b; Shimizu and Itakura, 1989), but computational costs may limit incorporation into the types of sedimentological models discussed here.

Local sorting of sediment in curved channel flows could be incorporated in future sedimentological modeling. Some attempts to address this have been undertaken in connection with existing flow models (Allen, 1970; Bridge, 1976,1977,1984a; S. Ikeda, 1989; Parker and Andrews, 1985).

The natural variability of flow has important implications with respect to channel flow and bedforms, bank erosion, and overbank sedimentation. Bedforms in channels change geometry as discharge changes, but with a lag in some cases (Allen, 1974). In the present model it is assumed that the response time of the large curvature-induced bedforms (point bars and related features) is slow enough that they change little during individual flow events and that the averaged response is the same as would be produced by a steady, *dominant* discharge, presumably a near-bankfull stage. The validity of this assumption can be tested by field study, appropriately scaled laboratory experiments or by computer experiments.

Bank Erosion Processes and Cut-offs

Although bank erosion rates are here assumed to be proportional to the near-bank velocity perturbation (equation (1.6)), the model incorporates the more general rate law incorporating a possible positive or negative contribution of the depth perturbation (equation (1.10)). As previously discussed, a variety of other assumptions might be appropriate.

The model can be extended to provide for both random and systematic spatial variations in bank erodibility, such as decreased erodibility of valley walls and clay

plugs deposited in cut-offs (Fisk, 1947). At present the model does provide for a finite valley width with walls of zero erodibility (Figure 1.5).

Bank erosion rates also are assumed to respond to a dominant discharge. Discharge variation affects not only the magnitude of the velocity and depth perturbations, but also their distribution around the bend (lags in response to curvature changes become greater at higher discharges). Variable discharge following a log-normal frequency distribution has been incorporated into an earlier version of the channel migration model. Preliminary experiments suggested that patterns of bank erosion and channel migration were not changed significantly by inclusion of variable discharge.

Neck cut-offs presently are assumed to occur when centerlines approach closer than a critical distance. However, stochastic modeling would be more realistic for neck cut-offs, with probabilities decreasing with greater neck width and increasing with higher discharges (Bridge, 1975).

The development of high sinuosity in meandering channels is restricted primarily by chute cut-offs. Chute cut-offs generally occur across recently deposited point bar and low floodplain deposits and the probability of their occurrence presumably increases the greater the decrease in bend length provided by the cut-off and the lower the elevation across the cut-off site. The probability also should depend upon main channel flow velocity and depth near the chute and the angle with which the upstream end of the chute intersects the main stream at its upstream end, decreasing in likelihood as the angle approaches 90° and proportionally less flow is diverted. Cut-offs are initiated primarily during high flows, although complete diversion is a slow process generally (Fisk, 1947; Bridge et al., 1986).

As discussed above, chute cut-offs are more common in streams with low rates of overbank sedimentation and a high width/depth ratio, and commonly occur along sloughs. Since the model simulates development of these sloughs, such cut-offs could be incorporated into the model realistically.

Avulsions are abandonment of long sections of an existing meander belt in favor of a more direct route across the existing floodplain. Avulsions are common only where the streams are aggrading relative to their floodplain (Allen, 1978; Leeder, 1978; Bridge and Leeder, 1979; Bridge, 1984b; Alexander and Leeder, 1987; Brizga and Findlayson, 1990), becoming the dominant mechanism of channel shifting on alluvial fans and river deltas. However, since such situations are required for preservation of thick meandering stream deposits, incorporation of avulsions into the model is desirable for sedimentological studies. Modeling of avulsions requires book-keeping of stream elevation changes relative to the floodplain, which could be done in an *ad hoc* manner (e.g. assuming a constant rate of rise) or by modeling the long-valley routing of bedload and regional elevation changes resulting from tectonic, sea-level, or consolidation processes. A simple implementation of avulsion probability would incorporate relative channel-floodplain elevations, bank and natural levee height, and possibly the magnitude of the sinuosity change and individual flood heights.

Deposition Modeling

The deposition rate laws incorporated equations (1.17) and (1.18) admittedly are crude, but they incorporate most of the features noted in empirical studies, including the role of channel bars and deposition rate decreasing with floodplain height and

distance from the main channel. Unfortunately, little published data exists for testing and refining of this model.

An obvious extension would be to include grain size and stratigraphic information by modeling deposit thickness, bedform, and grain size. Grain size and bedforms of point-bar deposits can be related to within-channel sorting and flow parameters much in the manner adopted by Allen (1970), Bridge (1975,1978,1984a) and Bridge and Jarvis (1977,1982). In overbank sedimentation each grain size range might be treated using a relationship such as equation (1.17) with varying parameters. For example, fine sizes would have large diffusion length, λ, and low intrinsic rate, μ, eliminating the need for a separate deposition rate of fine sediment, ν. This would yield the decreasing grain size with distance noted in overbank deposition (Fisk, 1947; Kesel et $al.$, 1974; Pizzuto, 1987).

Overbank sedimentation also may be different depending upon location inside versus outside of the nearest bend. This could be added by incorporating a multiplicative term $(1 + \sigma\, \eta_{1b})$ in equation (1.17), where σ is a scale factor to account for secondary current effects on sediment diffusion from the main channel. Fisk (1947) suggests that natural levees are more common on the outside of meander bends, suggesting a positive value for σ. This could result from the radially outward near-surface secondary flows within bends. However, the higher initial elevations of the older, eroding banks may enhance levee development relative to point bars. The higher near-bank bed elevations at point bars results from near-bed, inward secondary flows, which also enhance inward suspended load transport, suggesting the opposite sign for σ. It may be that σ changes sign from coarser to finer suspended load sizes.

Variations in discharge and associated flow depths are an essential control on overbank sedimentation. In the present model an averaged response to many over-bank flow events is assumed, which may be satisfactory for prediction of long-term deposition rates and resultant floodplain topography, but it is clearly inadequate for simulation of floodplain stratigraphy, which generally exhibits stratification resulting from individual flood events. Incorporation of overbank events would be fairly straightforward, with deeper flows corresponding to larger E_{max} (the water level), μ and λ in equation (1.17) for a given grain size range. For example, Pizzuto (1986) has modeled channel bank height as a function of the frequency distribution of flood depths and sediment loading, using an approach pioneered by Wolman and Leopold (1957).

Crevasse-splay deposits also could be incorporated as a stochastic model component, with initiation probability presumably a function of bank height, flood depth and possibly position within a bend. Similarly, scroll bar topography and deposits might be included in high-resolution floodplain modeling in an empirical fashion.

Deposition rates and grain sizes in the present model are parameterized by elevation and distance from the river, based upon a simple diffusional model of overbank sediment transport. However, as Pizzuto (1987) points out, advectional flow transport can lead to patterns of deposition rates and grain sizes not describable by the above parameters. This is particularly important for flows in chutes and sloughs, where both suspended load advection and bedload transport may occur. It may be possible to improve the model by empirical corrections, or overbank flow patterns and associated depositional processes might be included as an additional component if computational costs are not excessive. Techniques for modeling of overbank flows

have been developed (Knight and Demetriou, 1983; Yen and Yen, 1984; Ervine and Ellis, 1987; Knight, 1989; Gee, Anderson and Baird, 1990; Miller, 1990).

Very large floods may cause erosional and depositional features that clearly are outside the range of the present model framework. One such effect is widening of the main channel, which can be very dramatic where banks are readily eroded (Schumm and Lichty, 1963; Burkham, 1972; Osterkamp and Costa, 1987), sometimes resulting in a change of channel pattern from meandering to braided. Other effects include development of new chutes or re-excavation of old chutes, stripping of the floodplain surface, or deposition of a veneer of coarse gravel (Graf, 1983; Nanson, 1986; Ritter and Blakely, 1986; Baker, 1988; Kochel, 1988). However, such effects are most important in mountain or confined valleys and do not appear to be common in the classic meandering of the lowland rivers, which are also those that are most commonly represented in the stratigraphic record.

DISCUSSION: MODEL VALIDATION

The present model appears to replicate the major features of natural meandering streams. In addition, suggestions have been made to improve the fidelity of model representation of natural processes and deposits. However, despite many years of observations, relevant data for model validation, calibration and revision remains fragmentary and inconclusive. Further development of the model should proceed only hand-in-hand with field, laboratory, map, and theoretical work.

Field studies generally have involved investigation of one or, at most, a few meander bends, including studies of flow and sediment transport (Bathurst, 1979; Dietrich, Smith and Dunn, 1979; Bridge and Jarvis, 1982; Dietrich and Smith, 1983, 1984; Dietrich, 1987; Dietrich and Whiting, 1989), bank erosion processes (Hughes, 1977; Lawler, 1986a,b), channel and overbank sedimentation processes, and floodplain stratigraphy. Such studies have proven very useful in validation of theoretical models and elucidation of the types and rates of processes occurring in natural channels.

Laboratory studies (e.g. Fisk, 1947; Wolman and Brush, 1961; Hickin, 1969; R. Hooke, 1975; Desheng and Schumm, 1987; Odgaard and Bergs, 1988) offer controlled conditions useful for unraveling complicated process interactions and validation of theoretical models. However, time and costs limit the range of experiments, and certain processes, especially overbank sedimentation and effects of cohesive bank sediments, are difficult to scale to laboratory dimensions.

Theoretical models underpin quantitative prediction, simulation and interpretation of natural phenomena, but development of theory requires field or laboratory observations for validation, and theory may be limited in applicability owing to model shortcomings or computational costs.

Further development of simulation models requires quantitative studies of morphology, migration and deposition rates, as well as sedimentological and stratigraphic relationships, over spatial scales extending through several to dozens of meander bends and over temporal scales incorporating extensive channel shifting and associated deposition and cut-offs. Several crucial needs for studies at such *reach-length* spatio-temporal scales are discussed below.

Reach-Length Studies

Validation of Migration Model

The spatio-temporal pattern of channel migration depends both on the flow and transport model as well as the model for bank erosion. The combined assumptions used in the simulations clearly are sufficient to produce meander patterns that are visually similar to many meandering streams of high sinuosity. However, theoretical model development clearly has outpaced empirical validation. Two approaches that can be used to test theoretical models are (1) static comparison of simulated and natural meander planform geometry and (2) kinematic comparison of predicted and simulated channel migration.

Static Comparisons

Howard and Hemberger (in press) have developed a suite of 40 statistical variables to characterize meander morphometry. These include *ensemble* statistics based on measures of sinuosity, spectral characteristics, fitting of autoregressive models, and moments of channel curvature. In addition, *half-meander* statistics are based upon breaking the channel into individual half-meanders, or half-loops at inflection points and statistically characterizing their sinuosity, length, shape and asymmetry. These variables were measured on 57 long reaches of freely meandering channels from 33 rivers. In addition, these statistics also were measured on planforms generated by two theoretical models, the first being the disturbed periodic model (DPM) of Ferguson (1976,1977) (which stochastically generates meander planforms but does not simulate meander kinematics) and the second being the simulation model of Howard and Knutson (1984) (HKM) based upon the theoretical model of Ikeda, Parker and Sawai (1981).

Discriminant analysis is used to compare the natural streams with the two theoretical models (Figure 1.9). Two discriminant variables that are linear combinations of the suite of morphometric variables clearly are able to separate natural streams from the two theoretical models despite their visual similarity. The DPM and HKM simulated streams have less variability of centerline curvature for a comparable sinuosity and a narrower range of half-meander sizes than the natural streams. In addition, the HKM streams have more sinuous half-meanders, greater overall sinuosity, and more strongly asymmetrical meanders (upstream skewing) than natural streams. Although the statistical analysis clearly points out deficiencies in the theoretical models, the suite of variables are very sensitive to small systematic differences in morphometry, and the HKM model remains a good first approximation to natural meandering for highly sinuous streams.

There are several possible reasons for the morphometric differences between HKM simulated streams and natural streams:

(1) Random variations in bank erodibility were incorporated into some simulations with the HKM model, with little improvement in planform similarity to natural streams. However, systematic variations of bank erodibility occur in natural streams in that bank erosion may be hindered or stopped by natural levees and
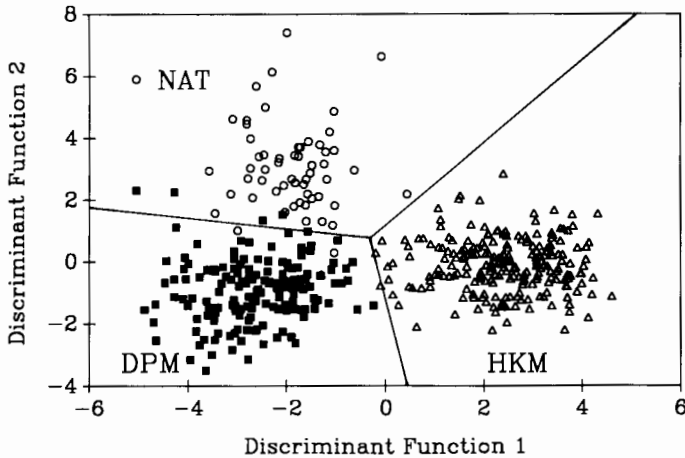
Figure 1.9 Scores for two discriminant functions of meander morphology for natural streams (NAT, open circles), streams simulated with the disturbed periodic model of Ferguson (1976; DPM, filled squares), and streams simulated with the kinematic model of Howard and Knutson (1984; HKM, open triangles). Discriminant boundary fences between the three classes of meanders are shown as the intersecting lines. Note that the two linear combinations of meander morphology indices produce almost complete discrimination between the three classes

exposure of clay plugs from old oxbow lakes (Fisk, 1947; H. Ikeda, 1989; Thorne, this volume). Such effects could be investigated in future revision of the model.

(2) Some natural meandering streams appear to have short meanders superimposed upon larger meanders, often generating the compound or cumuliform forms noted by Brice (1974a,b) and Hickin (1974). One cause may be temporal change in dominant wavelength, such as would result from a long-term decrease in flood peaks, so that short, new meanders develop on older, larger ones. Although this may occur on a few natural streams, a more universal cause may be the simultaneous operation of two distinct processes affecting meandering in streams. The first is the secondary circulation caused by stream curvature that is incorporated in the theory of Ikeda, Parker and Sawai (1981) and the HKM model. The second is the formation of alternate bars owing to sediment transport – flow interactions. Curvature-forced alternate bars are incorporated into the JP model used in the present simulations, but were not included in the HKM simulations used for the morphometric comparison. The inclusion of the curvature-forced bars allows for resonant interactions and overdeepening effects (Johannesson and Parker, 1989; Parker and Johannesson, 1989) that may have significant effects on meander morphometry. In addition, there may be additional systematic interactions between alternate bars and meander planform not accounted for in the JP model (including the locking of migrating bars in tight bends discussed above), as suggested by experiments (Whiting and Dietrich, 1989; Whiting, 1990).

(3) Bank erosion rates in the HKM model are assumed to be proportional to the velocity perturbation. As discussed above, a variety of other functional forms may occur. A few variations in the functional dependence of bank erosion rates with

the velocity and depth perturbations were incorporated in the HKM simulations used in the discriminant analysis, with no dramatic improvement of meander morphometrics compared with natural streams.

Kinematic Comparisons. Analysis of the kinematic pattern of channel migration of natural and simulated channels potentially is much more sensitive than the static comparisons and can offer important clues as to specific sources of model deficiencies. Unfortunately, although a rich data base of historical meander change exists, analyses of meander kinematics to date have been qualitative primarily or have yielded only summary statistics, such as average bank erosion rates (e.g. Brice, 1974a,b; Dort, 1978; Hooke, 1977,1979,1980,1984). Studies of the systematic variation in erosion rates with channel curvature and sediment properties have utilized isolated bends (Hickin and Nanson, 1975,1984; Nanson and Hickin, 1983, 1986), and have not accounted fully for upstream control of local flow and bed characteristics implied in theoretical models (such as the JP model used here) (Parker, 1984; Furbish, 1988). Howard and Knutson (1984) have used an earlier version of the flow model to simulate several decades of channel shifting on the White River of Indiana, with generally encouraging results. Short-term predictions of channel shifting also have been made by Parker (1982), Beck (1984), and Beck, Mefli and Yalamanchili (1984). The flow and transport model has been compared with flume studies of meandering channels (Johannesson and Parker, 1989). Pizzuto and Meckelnburg (1989), Hasegawa (1989a,b) and Furbish (1988) have compared observed bank erosion for individual bends or short reaches with model predictions. Although these comparisons generally are encouraging, they are too few and too rudimentary to comprise a thorough testing of the flow and erosion model. What is needed is systematic analysis of meander kinematics on a number of long reaches of natural and simulated channels and a comparison with model predictions.

Reach-length historical records of change of natural meandering channels can be used to test (or develop) predictive models of channel migration, involving both forward and inverse techniques.

Forward Analysis. The simplest forward method is to use theoretical models of flow and bend topography (such as the JP model) together with assumptions regarding an appropriate bank erosion rate law. A historical pattern of the river is used for initial conditions, and the simulation model predicts future migration, which can be compared with actual channel shifting. An appropriate criterion for degree of correspondence might be least-squares difference between the actual and predicted channel pattern. Cut-offs have to be treated specially, since either the predicted occurrence of a cut-off that did not occur or the reverse would lead automatically to very large least-squares discrepancies. Appropriate model parameters (e.g. F, β, γ, $\mathscr{E}$) can be estimated from field data. The disadvantage of this approach is that it is laborious to experiment with model parameters and bank erosion rate law assumptions to find the best fit to the observed changes.

A more flexible forward approach is to use the natural channel shift data to construct a spatial series of erosion rates together with the corresponding spatial series of channel curvatures. Because the channel is shifting through time, an

intermediate natural channel half-way between the initial and final locations must be constructed. These data can be used in several ways. The combined flow and bank erosion models can be used, with appropriate parameter assumptions, to estimate bank erosion rates for the intermediate channel planform. This approach gives the flexibility of examining the bank erosion model separately *assuming* that the flow and bed topography model is correct.

Inverse Analysis. Spatial series of bank erosion rates and curvature from natural streams, as discussed above, can be used in a variety of ways to fit 'time series' models to the observed data statistically. A variety of techniques have been developed to develop such models, the simplest of which are linear (Box and Jenkins, 1976). Transfer modeling techniques can be used to develop autoregressive and/or moving average (ARMA) models relating the time series of curvature and observed erosion rates. These linear models imply a governing differential equation whose parameters can be inferred from the fitted model. For example, the linear model of flow velocity and bank erosion of Ikeda, Parker and Sawai (1981) utilizes a single governing differential equation relating the curvature series to bank erosion rates. However, the multiple equation model of JP (Appendix A) could not be fit readily by ARMA transfer model techniques. However, an intermediate approach is again available if the JP model is used in a forward manner to predict velocity and depth perturbations, and transfer function techniques are used to derive an appropriate bank erosion model, including possible indentification of systematic spatial variations in bank erodibility, such as clay plugs.

Spatio-temporal information of neck and chute cut-offs and relevant information on point-bar heights, presence of sloughs, etc. also can be related to the spatial series of curvature and erosion rates in order to develop predictive models.

Validation of Deposition Model

The deposition model is the most difficult of the components to validate, because relevant data are difficult to obtain. The simplest type of quantitative comparisons between simulated and natural floodplains are statistics relating floodplain age, elevation and distance from stream channels. The analysis also could include as factors the position on inside or outside of bend and distance to abandoned channels. A few local studies have related floodplain elevation to age (Everitt, 1968; Kesel *et al.*, 1974; Nanson, 1980). However, reach-length measurements of floodplain elevations at sufficient vertical and horizontal resolution to be useful in model validation are rare. A few large rivers, notably the Mississippi, have been mapped at 5–10 ft contour intervals, but few reaches have slight enough influence of man (e.g. levee build-up, bank revetments, and artificial cut-offs) to form a useful data base. However, low-level stereo aerial photography is available for many rivers, and could be used to make detailed elevation measurements. Floodplain ages can be determined by dendrochronology (Everitt, 1968; Hickin and Nanson, 1975), although many rapidly meandering streams have sufficient historical record from maps and aerial photographs to be used to construct age maps.

Depositional features, such as point- and mid-channel bars, sloughs and floodplain, can be characterized by their morphometric or sedimentological characteristics (elevation, size, bedforms, grain size, etc.) and position along the channel, and related to the spatial series of curvature and erosion rates by time series analysis.

Information on floodplain sedimentology and stratigraphy is more difficult to obtain. Cores and trenches are the obvious but tedious method, supplemented with archaeological and age-dating techniques to provide rate information (e.g. Brakenridge, 1984,1985; Brown, 1987,1990; Walling and Bradley, 1989). Judicious use of sections exposed in cut banks also can be useful. Ancient deposits in the sedimentary record serve as comparisons. Relatively short duration studies of rates and spatial patterns of deposition and erosion are quite practical for reach-length studies, using surveying, coring and use of markers such as sand or gypsum.

CONCLUSIONS

The present model combines a model for flow and bed topography in meandering streams (Johannesson and Parker, 1989) with the assumption that bank erosion rates are related to the near-bank perturbations of downstream velocity and channel depth. This model provides realistic migration of simulated channels, although the simulated channels tend to be somewhat more asymmetric, sinuous and regular than natural channels.

The floodplain deposition model, which assumes that deposition rates decrease with distance from the closest channel and with increasing floodplain elevation, produces simulated topography that resembles that of natural floodplains, including point bars and oxbow lakes. Bank sedimentation is assumed to be initiated from the near-bank depths predicted by the flow-bed topography model. This produces linear depressions or sloughs at the downstream, inside margins of point-bar complexes in locations of sharp bends. Similar sloughs or mid-channel bars are found in natural channels at sharp bends, particularly at locations of confined meandering and recent cut-offs.

Both the meandering and depositional models can be modified in a number of ways to increase the range of features that are simulated (such as floodplain stratigraphy) or to improve the fidelity to natural processes. However, both existing model assumptions and suggested modifications will require validation through studies of natural meandering processes, particularly over reaches of several bends or more.

ACKNOWLEDGEMENTS

LIST OF SYMBOLS

A	coefficient of transverse bed slope	Equations (1.A5) and (1.A16)
C_f	coefficient of friction	Table 1.1
$\mathscr{C}$	Channel planform curvature (see Figure 1.1) (L^{-1})	Table 1.2
D	distance to nearest channel (L)	Equation (1.17)
E	elevation (L)	Equations (1.17) and (1.18)
$\mathscr{E}$	bank erodibility (LT^{-1})	Equation (1.3)
F	Froude number	Table 1.1
$\mathscr{F}(d)$	bank shear resistance, a function of median grain size, d, of sediment at base of cut bank $(ML^{-1}\,T^{-2})$	Equation (1.11)
g	gravitational acceleration (LT^{-2})	Table 1.1
h	local channel depth (see Figure 1.1) (L)	Equation (1.2)
H	section average channel depth (L)	Equation (1.2)
l	distance between nodes defining channel centerline (L)	Equation (1.16)
M	exponent relating sediment transport rate to velocity	Table 1.1
n	cross-stream distance from centerline (L)	Figure 1.1
s	downstream distance along centerline (L)	Figure 1.1
$\mathscr{T}$	sinuosity of channel reach	Equation (1.12)
u	local vertically-averaged velocity (LT^{-1})	Equation (1.1)
U	section average velocity (LT^{-1})	Equation (1.1)
W	channel width (L)	Table 1.1
Z	weighting coefficients for differentials	Equation (1.A19)
α	weighting coefficient for velocity for bank erosion	Equation (1.10)
β	transverse bed slope effect on transverse bedload transport	Table 1.1
γ	channel width/depth ratio	Table 1.1
Γ	parameter governing alternate bar wavelength	Equation (1.A7)
δ	parameter governing phase shift of secondary flow	Equation (1.A4)
ε	weighting coefficient of depth for bank erosion	Equation (1.10)
ζ	bank erosion rate (LT^{-1})	Equation (1.3)
η	bed elevation (L)	Figure 1.1
λ	characteristic diffusion scale length (L)	Equation (1.17)

μ	weighting coefficient for coarse-grained sediment deposition (T^{-1})	Equation (1.17)
ν	weighting coefficient for fine-grained sediment deposition (T^{-1})	Equation (1.17)
ζ	local water surface elevation (L)	Figure 1.1
π	dimensionless excess shear stress	Equation (1.7)
ϱ	fluid density (ML^{-3})	Table 1.1
τ	average bed shear stress $(ML^{-1}\,T^{-2})$	Equation (1.3)
Φ	floodplain deposition rate (LT^{-1})	Equation (1.17)
χ, χ_1, χ_{20}	velocity profile shape parameters	Equations (1.A1)–(1.A3)
Ψ	angle, in radians, between successive centerline nodes (see Figure 1.1)	Equation (1.16)

L, length; M, mass; T, time.

Subscripts
0 value for straight (non-sinuous) channel
1 dimensionless perturbation (except for χ_1)
b near-bank value at $n = W/2$
c value derived from curvature-forced solution with tractive force balance
f value correcting curvature-forced solution for sediment transport continuity (except for C_f)
d downstream value
i enumeration index
s variable expressing effect of secondary flow strength and phase shift
t value at threshold of erosion
u upstream value
w value non-dimensionalized by multiplying or dividing by channel width

APPENDIX A

The Johannesson–Parker Flow and Sediment Transport Model

The following parameters are defined in terms of the input parameters (Table 1.1) and used in the differential equations presented below:

$$\chi_1 = 0.077/C_f^{1/2} \qquad (1.A1)$$

$$\chi = \chi_1 - 1/3 \qquad (1.A2)$$

$$\chi_{20} = (\chi^3 + \chi^2 + 2\chi/5 + 2/35)/\chi_1^3 \qquad (1.A3)$$

$$\delta = \chi_1^2\,(\chi + 1/4)/(\chi^2/12 + 11\chi/360 + 1/504) \qquad (1.A4)$$

$$A = 2(\chi + 2/7)/(0.267\beta\,(\chi + 1/3)) \qquad (1.A5)$$

$$A_s = 724\,(2\chi^2 + 4\chi/5 + 1/15)/(\gamma^2\,\chi_1) \qquad (1.A6)$$

$$\Gamma = 4\beta/(\gamma^2\,C_f) \qquad (1.A7)$$

These terms are explained more fully in the List of Symbols.

As with channel depth and velocity, dimensionless perturbations of bed and water-surface elevations are defined:

$$\eta_1 = \eta/H \qquad\qquad\qquad (1.A8a)$$

$$\zeta_1 = \zeta/H \qquad\qquad\qquad (1.A8b)$$

These differ from the depth and velocity perturbation definitions (equations (1.1) and (1.2)) because the mean values of η and ζ are zero.

Depth, velocity and bed-elevation perturbations are resolved into a component resulting from curvature effects (subscript c) and a correction accounting for sediment transport continuity (subscript f):

$$u_{1b} = u_{1cb} + u_{1fb} \qquad\qquad\qquad (1.A9)$$

$$h_{1b} = h_{1cb} + h_{1fb} \qquad\qquad\qquad (1.A10)$$

$$\eta_{1b} = \eta_{1cb} + \eta_{1fb} \qquad\qquad\qquad (1.A11)$$

The basic differential equations that must be solved are presented below. The equations are equivalent to the JP equations, but are normalized by channel width rather than half-width, maximum curvature and wavenumber as in JP. The three equations given below must be solved sequentially in order to determine the velocity perturbations:

$$\frac{d\,\mathscr{C}_{ws}}{dS_w} + \delta\gamma\, C_f\, \mathscr{C}_{ws} = \delta\gamma\, C_f\, \mathscr{C}_w \qquad\qquad (1.A12)$$

$$\frac{\partial u_{1cb}}{\partial S_w} + 2\gamma\, C_f\, u_{1cb} = 0.5 \left\{ -\chi_{20}\, \frac{\partial\,\mathscr{C}_w}{\partial S_w} + \gamma\, C_f \left[(F^2\,\chi_{20} - 1)\, \mathscr{C}_w \right.\right.$$

$$\left.\left. + (A + A_s)\, \mathscr{C}_{ws} \right] \right\} \qquad\qquad (1.A13)$$

$$\frac{\partial^2 u_{1fb}}{\partial S_w^2} + \gamma\, C_f\, [3 - M + (\pi/2)^2\, \Gamma]\, \frac{\partial u_{1fb}}{\partial S_w} + 2\,[\gamma\, C_f\, (\pi/2)]^2\, \Gamma\, u_{1fb} =$$

$$\gamma\, C_f\, (M - 1)\, \frac{\partial u_{1cb}}{\partial S_w} - 0.5\gamma\, C_f \left[F^2\, \chi_{20}\, \frac{\partial\mathscr{C}_w}{\partial S_w} + A\, \frac{\partial\,\mathscr{C}_{ws}}{\partial S_w} \right] \qquad (1.A14)$$

Having solved for velocity using equations (1.A12)–(1.A14), the following equations give the depth perturbations:

$$\eta_{1fb} = -\,[1/(\gamma\, C_f)]\, \frac{\partial u_{1fb}}{\partial S_w} - 2\, u_{1fb} \qquad\qquad (1.A15)$$

$$\eta_{1cb} = -0.5\, A\, \mathscr{C}_{ws} \qquad\qquad\qquad (1.A16)$$

$$\zeta_{1b} = 0.5\, F^2\, \chi_{20}\, \mathscr{C}_w \qquad\qquad\qquad (1.A17)$$

$$h_{1b} = \zeta_{1b} - \eta_{1b} \qquad\qquad\qquad (1.A18)$$

The solution for these equations marches downstream. First and second derivatives are expressed as a weighted sum of the local ($i = 0$) and upstream ($i > 0$) values of the differentiated variable, using formulae for asymmetric differentials. For example, $d\,\mathscr{C}_{ws}/dS_w$ becomes

$$d\,\mathscr{C}_{ws}/dS_w = \sum_{i=0}^{n} \mathscr{C}_{ws_i} Z_i, \qquad (1.A19)$$

where Z_i are functions of the upstream distances S_{wi} to the stream nodes.

The Z_i are found by the method of undetermined coefficients (Gerald and Wheatley, 1989, their Appendix B) through solution of simultaneous equations (the Z_i are different for each location and iteration since the S_{w_i} vary downstream and temporally). The resulting difference equation is solved for the unknown local value ($\mathscr{C}_{ws_0}$ in this case). The number of polynomial terms, n, is specified (typically four or five). This autoregressive approach has been suggested by Furbish (1988,1989) and is equivalent functionally to the convolution approach used by Howard and Knutson (1984) and Johannesson and Parker (1989).

For the first few stream locations (when there are less than n upstream points) the derivatives are set to zero. This means that a lead-in section of stream is required in order to obtain good estimates of the variables, ideally, one or more meander wavelengths long.

REFERENCES

Akky, M. R. and C. K. Shen (1973). Erodibility of a cement-stabilized sandy soil. In *Soil Erosion: Causes and Mechanisms*, US Highway Research Board Special Report 135, pp. 30–41.

Alexander, J. and M. R. Leeder (1987). Active tectonic control on alluvial architecture. In F. G. Ethridge, R. M. Flores and M. D. Harvey (eds), *Recent Developments in Fluvial Sedimentology*, Society of Economic Paleontologists and Mineralogists, Special Publication No. 39, pp. 243–252.

Allen, J. R. L. (1970). A quantitative model of grain size and sedimentary structures in lateral deposits. *Geological Journal*, 7, 129–146.

Allen, J. R. L. (1974). Reaction, relaxation, and lag in natural sedimentary systems: general principles, examples and lessons. *Earth Science Reviews*, 10, 263–342.

Allen, J. R. L. (1977). Changeable rivers: some aspects of their mechanics and sedimentation. In K. J. Gregory, (ed.), *River Channel Changes*, Wiley, pp. 15–45.

Allen, J. R. L. (1978). Studies in fluviatile sedimentation: an exploratory quantitative model for the architecture of avulsion-controlled alluvial suites. *Sedimentary Geology*, 21, 129–147.

Allen, J. R. L. (1982). Free meandering channels and lateral deposits. In *Sedimentary Structures: Their Character and Physical Basis*, Vol. 2, Elsevier, pp. 53–100.

Ariathurai, R. and K. Arulandan (1986). Erosion rates of cohesive soils. *Journal of the Hydraulics Division, American Society of Civil Engineers*, 104, 279–298.

Baker, V. R. (1988). Flood erosion. In V. R. Baker, R. C. Kochel and P. C. Patton (eds), *Flood Geomorphology*, Wiley, pp. 123–137.

Bathurst, J. C. (1979). Distribution of boundary shear stress in rivers. In D. D. Rhodes and G. P. Williams (eds), *Adjustments of the Fluvial System*, Kendall/Hunt, pp. 95–116.

Beck, S. (1984). Mathematical modeling of meander interaction. In C. M. Elliott (ed.), *River Meandering*, American Society of Civil Engineers, pp. 932–941.

Beck, S., D. A. Mefli and K. Yalamanchili (1984). Lateral migration of the Genessee River, New York. In C. M. Elliott (ed.), *River Meandering*, American Society of Civil Engineers, pp. 510–517.

Blondeaux, P. and G. Seminara (1985). A unified bar-bend theory of river meanders. *Journal of Fluid Mechanics*, **157**, 449–470.

Bluck, B. J. (1976). Sedimentation in some Scottish rivers of low sinuosity. *Transactions, Royal Society of Edinburgh*, **69**, 425–456.

Box, G. E. P. and G. M. Jenkins (1976). *Time Series Analysis: Forecasting and Control*, Holden-Day, 575 pp.

Brakenridge, G. R. (1984). Alluvial stratigraphy and radiocarbon dating along the Duck River, Tennessee: implications regarding flood-plain origin. *Geological Society of America Bulletin*, **95**, 9–25.

Brakenridge, G. R. (1985). Rate estimates for lateral bedrock erosion based on radiocarbon ages, Duck River, Tennessee. *Geology*, **13**, 111–114.

Brice, J. C. (1964). Channel patterns and terraces of the Loup Rivers in Nebraska. *U. S. Geological Survey Professional Paper*, **422-D**, 41 pp.

Brice, J. C. (1974a). Meandering pattern of the White River in Indiana – an analysis. In M. Morisawa (ed.), *Fluvial Geomorphology*, State University of New York, pp. 178–200.

Brice, J. C. (1974b). Evolution of meander loops. *Geological Society of America Bulletin*, **85**, 581–586.

Bridge, J. S. (1975). Computer simulation of sedimentation in meandering streams. *Sedimentology*, **22**, 3–43.

Bridge, J. S. (1976). Bed topography and grain size in open channel bends. *Sedimentology*, **23**, 407–414.

Bridge, J. S. (1977). Flow, bed topography, grain size and sedimentary structure in open channel bends: a three-dimensional approach. *Earth Surface Processes*, **2**, 401–416.

Bridge, J. S. (1978). Palaeohydraulic interpretation using mathematical models of contemporary flow and sedimentation in meandering channels. In A. D. Miall (ed.), *Fluvial Sedimentology*, Canadian Society of Petroleum Geologists, pp. 723–742.

Bridge, J. S. (1984a). Flow and sedimentary processes in river bends: comparison of field observations and theory. In C. M. Elliott (ed.), *River Meandering*, American Society of Civil Engineers, pp. 857–872.

Bridge, J. S. (1984b). Large-scale facies sequences in alluvial overbank environments. *Journal of Sedimentary Petrology*, **54**, 583–588.

Bridge, J. S. (1985). Paleochannel patterns inferred from alluvial deposits: a critical evaluation. *Journal of Sedimentary Petrology*, **55**, 579–589.

Bridge, J. S. and J. Jarvis (1977). Velocity profiles and bed shear stress over various bed configurations in a river bend. *Earth Surface Processes*, **2**, 281–294.

Bridge, J. S. and J. Jarvis (1982). The dynamics of a river bend: a study of flow and sedimentary processes. *Sedimentology*, **29**, 499–541.

Bridge, J. S. and M. R. Leeder (1979). A simulation model of alluvial stratigraphy. *Sedimentology*, **26**, 617–644.

Bridge, J. S., N. D. Smith, F. Trent, S. L. Gabel and P. Bernstein (1986). Sedimentology and morphology of a low-sinuosity river: Calamus River, Nebraska Sand Hills. *Sedimentology*, **33**, 851–870.

Brizga, S. O. and B. L. Findlayson (1990). Channel avulsion and river metamorphosis: the case of the Thompson River, Victoria, Australia. *Earth Surface Processes and Landforms*, **15**, 391–404.

Brown, A. G. (1987). Holocene floodplain sedimentation and channel response of the lower River Severn, United Kingdom. *Zeitschrift fur Geomorphologie*, **31**, 293–310.

Brown, A. G. (1990). Holocene floodplain diachronism and inherited downstream variations in fluvial processes: a study of the river Perry, Shropshire, England. *Journal of Quaternary Science*, **5**, 39–51.

Burkham, D. E. (1972). Channel changes of the Gila River in Safford Valley, Arizona 1846–1970. *U. S. Geological Survey Professional Paper*, **655-G**, 24 pp.

Callander, R. A. (1978). River meandering. *Annual Review of Fluid Mechanics*, **10**, 129–158.

Carey, W. C. (1969). Formation of flood plain lands. *Journal of the Hydraulics Division, Proceedings of the American Society of Civil Engineers*, **95**, 981–994.

Carson, M. A. and M. F. Lapointe (1983). The inherent asymmetry of river meanders. *Journal of Geology*, **91**, 41–55.

Colombini, M., G. Seminara and M. Tubino (1987). Finite-amplitude alternate bars. *Journal of Fluid Mechanics*, **181**, 213–232.

Desheng, J. and S. A. Schumm (1987). A new technique for modeling river morphology. In V. Gardiner (ed.), *International Geomorphology 1986*, Wiley, pp. 681–690.

Dietrich, W. E. (1987). Mechanics of flow and sediment transport in river bends. In K. S. Richards (ed.), *River Channels: Environment and Process*, Basil Blackwell, pp. 179–227.

Dietrich, W. E. and J. D. Smith (1983). Influence of the point bar on flow through curved channels. *Water Resources Research*, **19**, 1173–1192.

Dietrich, W. E. and J. D. Smith (1984). Bedload transport in a river meander. *Water Resources Research*, **20**, 1355–1380.

Dietrich, W. E. and P. Whiting (1989). Boundary shear stress and sediment transport in river meanders of sand and gravel. In S. Ikeda and G. Parker (eds), *River Meandering*, Water Resources Monograph 12, American Geophysical Union, pp. 1–50.

Dietrich,, W. E., J. D. Smith and T. Dunne (1979). Flow and sediment transport in a sand bedded meander. *Journal of Geology*, **87**, 305–314.

Dort, W. Jr. (1978). *Channel Migration Investigation: Historic Channel Change Maps, Kansas City District*, U. S. Army Corps of Engineers, 50 pp.

Ervine, D. A. and J. Ellis (1987). Experimental and computational aspects of overbank floodplain flow. *Transactions of the Royal Society of Edinburgh: Earth Sciences*, **78**, 315–325.

Everitt, B. L. (1968). Use of the cottonwood in an investigation of the recent history of a flood plain. *American Journal of Science*, **266**, 417–439.

Ferguson, R. I. (1976). Disturbed periodic model for river meanders. *Earth Surface Processes*, **1**, 337–347.

Ferguson, R. I. (1977). Meander migration: equilibrium and change. In K. J. Gregory (ed.), *River Channel Changes*, Wiley, pp. 235–263.

Fisk, H. N. (1947). *Fine-Grained Alluvial Deposits and their Effect on Mississippi River Activity*, Waterways Experiment Station, U. S. Army Corps of Engineers, 82 pp.

Fredsoe, J. (1978). Meandering and braiding of rivers. *Journal of Fluid Mechanics*, **84**, 609–624.

Friedkin, J. F. (1945). *A Laboratory Study of the Meandering of Alluvial Rivers*, Mississippi River Commission, Waterways Experiment Station, U. S. Army Corps of Engineers, 40 pp.

Fukuoka, S. (1989). Finite amplitude development of alternate bars. In S. Ikeda and G. Parker (eds), *River Meandering*, Water Resources Monograph 12, American Geophysical Union, pp. 237–266.

Furbish, D. J. (1988). River-bed curvature and migration: how are they related? *Geology*, **16**, 752–755.

Furbish, D. J. (1989). The relation of thalweg position to channel curvature along the Ohio River. *Southeastern Geology*, **29**, 143–154.

Gee, D. M., M. G. Anderson and L. Baird (1990). Large-scale floodplain modeling. *Earth Surface Processes and Landforms*, **15**, 513–523.

Gerald, C. F. and P. O. Wheatley (1989). *Applied Numerical Analysis*, Addison-Wesley, 679 pp.

Goss, D. W. (1973). Relation of physical and mineralogical properties to streambank stability. *Water Resources Bulletin*, **9**, 140–144.

Graf, W. L. (1983). Flood-related channel change in an arid-region river. *Earth Surface Processes and Landforms*, **8**, 125–139.

Grissinger, E. H. (1966). Resistance of selected clay systems to erosion by water. *Water Resources Research*, **2**, 131–138.

Grissinger, E. H. (1982). Bank erosion of cohesive materials. In R. D. Hey, J. C. Bathurst and C. R. Thorne (eds), *Gravel-bed Rivers*, Wiley, pp. 273–287.

Hasegawa, K. (1989a). Studies on qualitative and quantitative prediction of meander channel

shift. In S. Ikeda and G. Parker (eds), *River Meandering*, Water Resources Monograph 12, American Geophysical Union, pp. 215–236.

Hasegawa, K. (1989b). Universal bank erosion coefficient for meandering rivers. *Journal of Hydraulic Engineering*, **115**, 744–765.

Hickin, E. J. (1969). A newly-identified process of point bar formation in natural streams. *American Journal of Science*, **267**, 999–1010.

Hickin, E. J. (1974). Development of meanders in natural river-channels. *American Journal of Science*, **274**, 414–442.

Hickin, E. J. (1979). Concave-bank benches in the Squamish River, British Columbia, Canada. *Canadian Journal of Earth Science*, **16**, 200–203.

Hickin, E. J. and G. C. Nanson (1975). Character of channel migration on the Beatton River, northwest British Columbia, Canada. *Geological Society of America Bulletin*, **86**, 487–494.

Hickin, E. J. and G. C. Nanson (1984). Lateral migration rates of river bends. *Journal of Hydraulic Engineering*, **110**, 1557–1567.

Hooke, J. M. (1977). The distribution and nature of changes in river channel patterns: the example of Devon. In K. J. Gregory (ed.), *River Channel Changes*, Wiley, pp. 265–280.

Hooke, J. M. (1979). An analysis of the processes of river bank erosion. *Journal of Hydrology*, **42**, 39–62.

Hooke, J. M. (1980). Magnitude and distribution of rates of river bank erosion. *Earth Surface Processes*, **5**, 143–157.

Hooke, J. M. (1984). Meander behavior in relation to slope characteristics. In C. M. Elliott (ed.), *River Meandering*, American Society of Civil Engineers, pp. 67–76.

Hooke, J. M. (1986). The significance of mid-channel bars in an active meandering river. *Sedimentology*, **33**, 839–850.

Hooke, R. Le B (1975). Distribution of sediment transport and shear stress in a meander bend. *Journal of Geology*, **83**, 543–565.

Howard, A. D. (1984). Simulation model of meandering. In C. M. Elliott (ed.), *River Meandering*, American Society of Civil Engineers, pp. 952–963.

Howard, A. D. and Hemberger, A. T. (in press). Multivariate characterization of meandering. *Geomorphology*.

Howard, A. D. and G. Kerby (1983). Channel changes in badlands. *Geological Society of America Bulletin*, **94**, 739–752.

Howard, A. D. and T. R. Knutson (1984). Sufficient conditions for river meandering: a simulation approach. *Water Resources Research*, **20**, 1659–1667.

Howard, A. D., J. B. Morton, M. Gad-el-Hak and D. B. Pierce (1978). Sand transport model of barchan dune equilibrium. *Sedimentology*, **25**, 307–338.

Hughes, D. J. (1977). Rates of erosion on meander arcs. In K. J. Gregory (ed.), *River Channel Changes*, Wiley, pp. 193–205.

Ikeda, H. (1989). Sedimentary controls on channel migration and origin of point bars in sand-bedded meandering rivers. In S. Ikeda and G. Parker (eds), *River Meandering*, Water Resources Monograph 12, American Geophysical Union, pp. 51–68.

Ikeda, S. (1989). Sediment transport and sorting in bends. In S. Ikeda and G. Parker (eds), *River Meandering*, Water Resources Monograph 12, American Geophysical Union, pp. 103–126.

Ikeda, S., G. Parker and K. Sawai (1981). Bend theory of river meanders, 1, linear development. *Journal of Fluid Mechanics*, **112**, 363–377.

Jackson, R. G., II (1976). Depositional model of point bars in the lower Wabash River. *Journal of Sedimentary Petrology*, **46**, 579–594.

Johannesson, J. and Parker, G. (1989). Linear theory of river meanders. In S. Ikeda and G. Parker (eds), *River Meandering*, Water Resources Monograph 12, American Geophysical Union, pp. 181–214.

Kesel, R. H., K. C. Dunne, R. C. McDonald, K. R. Allison and B. E. Spicer (1974). Lateral erosion and overbank deposition on the Mississippi River in Louisiana caused by 1973 flooding. *Geology*, **2**, 461–464.

Kinoshita, R. (1961). *Investigation of channel deformation in Ishikari River*, Report of Bureau of Resources, Department of Science and Technology, Japan (in Japanese), 174 pp.

Knight, D. W. (1989). Hydraulics of flood channels. In K. Beven and P. Carling (eds), *Floods: Hydrological, Sedimentological and Geomorphological Implications*, Wiley, pp. 83–105.

Knight, D. W. and J. D. Demetriou (1983). Flood plain and main channel flow interaction. *Journal of the Hydraulics Division, Proceedings of the American Society of Civil Engineers*, **109**, 1073–1082.

Kochel, R. C. (1988). Geomorphic impact of large floods: review and new perspectives on magnitude and frequency. In V. R. Baker, R. C. Kochel and P. C. Patton (eds), *Flood Geomorphology*, Wiley, pp. 169–187.

Kondrat'yev, N. Ye (1968). Hydromorphological principles of computations of free meandering. 1. Signs and indices of free meandering. *Soviet Hydrology: Selected Papers*, **4**, 309–335.

Kuijper, C., J. M. Cornelisse and J. C. Winterwerp (1989). Research on erosive properties of cohesive sediments. *Journal of Geophysical Research*, **94**, 14341–14350.

Kulemina, N. M. (1973). Some characteristics of the process of incomplete meandering of the channel of the upper Ob' River. *Soviet Hydrology: Selected Papers*, **6**, 518–534.

Lapointe, M. F. and M. A. Carson (1986). Migration patterns of an asymmetric meandering river: the Rouge River, Quebec. *Water Resources Research*, **22**, 731–743.

Laury, R. L. (1971). Stream bank failure and rotational slumping: preservation and significance in the geologic record. *Geological Society of American Bulletin*, **82**, 1251–1266.

Lawler, D. M. (1986a). Bank erosion and frost action: an example from South Wales. In V. Gardiner (ed.), *International Geomorphology 1986*, Wiley, pp. 575–590.

Lawler, D. M. (1986b). River bank erosion and the influence of frost: a statistical examination. *Transactions of the Institute of British Geographers, N. S.* **11**, 227–242.

Leeder, M. R. (1978). A quantitative stratigraphic model for alluvium, with special reference to channel deposit density and interconnectedness. In A. D. Miall (ed.), *Fluvial Sedimentology*, Canadian Society of Petroleum Geologists, pp. 587–596.

Leopold, L. B. and M. G. Wolman (1957). River channel patterns—braided, meandering, and straight. *U. S. Geological Survey Professional Paper*, **282-B**, 85 pp.

Lewin, J. (1976). Initiation of bed forms and meanders in coarse-grained sediment. *Geological Society of America Bulletin*, **87**, 281–285.

Lewin, J. (1978). Meander development and floodplain sedimentation: a case study from mid-Wales. *Geological Journal*, **13**, 25–36.

Lewin, J. and B. J. Brindle (1977). Confined meanders. In K. J. Gregory (ed.), *River Channel Changes*, Wiley, pp. 221–233.

Lewis, G. W. and J. Lewin (1983). Alluvial cut-offs in Wales and the Borderlands. In *Modern and Ancient Fluvial Systems*, Blackwell Scientific Publications, pp. 145–154.

Miller, A. J., and M. G. Wolman (1990) 2D simulation of flood flow patterns in mountain valleys. *EOS (Transactions of the American Geophysical Union)*, **71**, 510.

Murray, W. A. (1977). Erodibility of coarse and sand-clayey silt mixtures. *Journal of the Hydraulics Division, Proceedings of the American Society of Civil Engineers*, **103**, 1222–1227.

Nanson, G. C. (1980). Point bar and floodplain formation of the meandering Beatton River, northeastern British Columbia, Canada. *Sedimentology*, **27**, 3–29.

Nanson, G. C. (1986). Episodes of vertical accretion and catastrophic stripping: a model of disequilibrium flood plain development. *Geological Society of America Bulletin*, **97**, 1467–1475.

Nanson, G. C. and E. J. Hickin (1983). Channel migration and incision on the Beatton River. *Journal of Hydraulic Engineering*, **109**, 327–337.

Nanson, G. C. and E. J. Hickin (1986). A statistical analysis of bank erosion and channel migration in western Canada. *Geological Society of America Bulletin*, **97**, 497–504.

Nanson, G. and K. Page (1983). Lateral accretion of fine-grained concave benches on meandering rivers. In *Modern and Ancient Fluvial Systems*, Blackwell Scientific Publications, pp. 133–143.

Neill, C. R. (1984). Bank erosion vs. bedload transport in a gravel river. In C. M. Elliott (ed.), *River Meandering*, American Society of Civil Engineers, pp. 204–211.

Nelson, J. M. and J. D. Smith (1989a). Flow in meandering channels with natural topography. In S. Ikeda and G. Parker (eds), *River Meandering*, Water Resources Monograph 12, American Geophysical Union, pp. 69–102.

Nelson, J. M. and J. D. Smith (1989b). Evolution and stability of erodible channel beds. In S. Ikeda and G. Parker (eds), *River Meandering*, Water Resources Monograph 12, American Geophysical Union, pp. 321–378.

Odgaard, A. J. (1987). Streambank erosion along two rivers in Iowa. *Water Resources Research*, **23**, 1225–1236.

Odgaard, A. J. (1989a). River-meander model. I: development. *Journal of Hydraulic Engineering*, **115**, 1433–1450.

Odgaard, A. J. (1989b). River-meander model. II: applications. *Journal of Hydraulic Engineering*, **115**, 1451–1464.

Odgaard, A. J. and M. A. Bergs (1988). Flow processes in a curved alluvial channel. *Water Resources Research*, **24**, 45–56.

Osman, A. M. and C. R. Thorne (1988). Riverbank stability analysis. I: development. *Journal of Hydraulic Engineering*, **114**, 134–150.

Osterkamp, W. R. and J. E. Costa (1987). Changes accompanying an extra-ordinary flood on a sand-bed stream. In L. Mayer and D. Nash (eds), *Catastrophic Flooding*, Allen & Unwin, pp. 201–224.

Parchure, T. M. and A. J. Mehta (1985). Erosion of soft cohesive sediment deposits. *Journal of the Hydraulics Division, American Society of Civil Engineers*, **111**, 1308–1326.

Parker, G. (1976). On the cause and characteristic scales of meandering and braiding in rivers. *Journal of Fluid Mechanics*, **76**, 457–480.

Parker, G. (1982). *Stability of the Channel of the Minnesota River Near State Bridge No. 93, Minnesota*, Project Report No. 205, St. Anthony Falls Hydraulic Laboratory, University of Minnesota, 33 pp.

Parker, G. (1984). Theory of meander bend deformation. In C. M. Elliott (ed.), *River Meandering*, American Society of Civil Engineers, pp. 722–732.

Parker, G. and E. D. Andrews (1985). Sorting of bed load sediment by flow in meander bends. *Water Resources Research*, **21**, 1361–1373.

Parker, G. and E. D. Andrews (1986). On the time development of meander bends. *Journal of Fluid Mechanics*, **162**, 139–156.

Parker, G. and H. Johannesson (1989). Observations on several recent theories of resonance and overdeepening in meandering channels. In S. Ikeda and G. Parker (eds), *River Meandering*, Water Resources Monograph 12, American Geophysical Union, pp. 379–416.

Parthenaides, E. (1965). Erosion and deposition of cohesive soils. *Journal of the Hydraulics Division, American Society of Civil Engineers*, **91**, 105–139.

Parthenaides, E. and R. R. Paaswell (1970). Erodibility of channels with cohesive boundaries. *Journal of the Hydraulics Division, American Society of Civil Engineers*, **96**, 755–771.

Pizzuto, J. E. (1984). Bank erodibility of sand-bed streams. *Earth Surface Processes and Landforms*, **9**, 113–124.

Pizzuto, J. E. (1986). Flow variability and bankfull depth of sand-bed rivers of the American Midwest. *Earth Surface Processes and Landforms*, **11**, 441–450.

Pizzuto, J. E. (1987). Sediment diffusion during overbank flows. *Sedimentology*, **34**, 301–317.

Pizzuto, J. E. and T. S. Meckelnburg (1989). Evaluation of a linear bank erosion equation. *Water Resources Research*, **25**, 1005–1013.

Ritter, D. F. and D. S. Blakely (1986). Localized catastrohic disruption of the Gasconade River flood plain during the December 1982 flood, southeast Missouri. *Geology*, **14**, 472–476.

Rohrer, W. L. (1984). Effects of flow and bank material on meander migration in alluvial rivers. In C. M. Elliott (ed.), *River Meandering*, American Society of Civil Engineers, pp. 770–782.

Schumm, S. A. and R. W. Lichty (1963). Channel widening and floodplain constriction along Cimarron River in southwestern Kansas. *U. S. Geological Survey Professional Paper*, **352-D**, 71–88.

Seminara, G. and M. Tubino (1989). Alternate bars and meandering: free, forced and mixed interactions. In S. Ikeda and G. Parker (eds), *River Meandering*, Water Resources Monograph 12, American Geophysical Union, pp. 267–320.

Shimizu, Y. and T. Itakura (1989). Calculation of bed variation in alluvial channels. *Journal of Hydraulic Engineering*, **115**, 367–384.

Taylor, G. and K. D. Woodyer (1978). Bank deposition in suspended-load streams. In A. D. Miall (ed.), *Fluvial Sedimentology*, Canadian Society of Petroleum Geologists, pp. 257–275.

Thorne, C. R. (1982). Processes and mechanisms of river bank erosion. In R. D. Hey, J. C. Bathurst, and C. E. Thorne (eds), *Gravel-bed Rivers*, Wiley, pp. 227–272.

Thorne, C. R. and J. Lewin (1979). Bank processes, bed material movement, and planform development in a meandering river. In D. D. Rhodes and G. P. Williams (eds), *Adjustments of the Fluvial System*, Kendall/Hunt, pp. 117–137.

Thorne, C. R. and Osman, A. M. (1988). Riverbank stability analysis. II: applications. *Journal of Hydraulic Engineering*, **114**, 151–172.

Thorne, C. R. and N. K. Tovey (1981). Stability of composite river banks. *Earth Surface Processes and Landforms*, **6**, 469–484.

Tubino, M. and G. Seminara (1990). Free-forced interactions in developing meanders and suppression of free bars. *Journal of Fluid Mechanics*, **214**, 131–159.

Turbull, W. J., E. L. Krinitsky and F. J. Weaver (1966). Bank erosion in the soils of the Lower Mississippi River. *Journal of Soil Mechanics and Foundation Engineering*, **92**, 121–137.

Ullrich, C. R., D. J. Hagerty and R. W. Holmberg (1986). Surficial failures of alluvial stream banks. *Canadian Geotechnical Journal*, **23**, 304–316.

Walling, D. E. and S. B. Bradley (1989). Rates and patterns of contemporary floodplain sedimentation: a case study of the river Culm, Devon, UK. *Geojournal*, **19.1**, 53–62.

Whiting, P. J. (1990). *Bar development and channel morphology*, Unpublished PhD dissertation, University of California, 196 pp.

Whiting, P. J. and W. E. Dietrich (1989). Multiple bars in highly sinuous flume bends: implications for bank erosion. *EOS (Transactions of the American Geophysical Union)*, **70**, 329.

Willis, B. J. (1989). Palaeochannel reconstructions from point bar deposits: a three-dimensional perspective. *Sedimentology*, **36**, 757–766.

Wolman, M. G. (1959). Factors influencing erosion of a cohesive river bank, *American Journal of Science*, **257**, 204–216.

Wolman, M. G. and L. B. Leopold (1957). River flood plains: some observations on their formation. *U. S. Geological Survey Professional Paper*, **282**-C, 87–109.

Wolman, M. G. and L. M. Brush, Jr. (1961). Factors controlling the size and shape of stream channels in coarse noncohesive sands. *U. S. Geological Survey Professional Paper*, **282-G**, 183–210.

Woodyer, K. D. (1975). Concave-bank benches on Barwon River, N. S. W. *Australian Geographer*, **13**, 36–40.

Yen, B. C. and C.-L. Yen (1984). Flood flow over meandering channels. In C. M. Elliott (ed.), *River Meandering*, American Society of Civil Engineers, pp. 554–561.